International Journal of Biological Macromolecules 272 (2024) 132722

Contents lists available at ScienceDirect

International Journal of Biological Macromolecules

journal homepage: www.elsevier.com/locate/ijbiomac

A comprehensive method for the sequential separation of extracellular xylanases and β-xylosidases/arabinofuranosidases from a new *Fusarium* species

Andrea Rodríguez-Sanz [a], Clara Fuciños [a], Célia Soares [b,c], Ana M. Torrado [a], Nelson Lima [b,c], María L. Rúa [a,*]

[a] Biochemistry Laboratory, Department of Analytical and Food Chemistry, University of Vigo, Ourense, Spain
[b] CEB-Biological Engineering Centre, University of Minho, Campus de Gualtar, Braga, Portugal
[c] LABBELS-Associate Laboratory, Braga, Guimarães, Portugal

ARTICLE INFO

Keywords:
Fusarium pernambucanum
Trifunctional
Xylanolytic enzyme

ABSTRACT

Several fungal species produce diverse carbohydrate-active enzymes useful for the xylooligosaccharide biorefinery. These enzymes can be isolated by different purification methods, but fungi usually produce other several compounds which interfere in the purification process. So, the present work has three interconnected aims: (i) compare β-xylosidase production by *Fusarium pernambucanum* MUM 18.62 with other crop pathogens; (ii) optimise *F. pernambucanum* xylanolytic enzymes expression focusing on the pre-inoculum media composition; and (iii) design a downstream strategy to eliminate interfering substances and sequentially isolate β-xylosidases, arabinofuranosidases and *endo*-xylanases from the extracellular media. *F. pernambucanum* showed the highest β-xylosidase activity among all the evaluated species. It also produced *endo*-xylanase and arabinofuranosidase. The growth and β-xylosidase expression were not influenced by the pre-inoculum source, contrary to *endo*-xylanase activity, which was higher with xylan-enriched agar. Using a sequential strategy involving ammonium sulfate precipitation of the extracellular interferences, and several chromatographic steps of the supernatant (hydrophobic chromatography, size exclusion chromatography, and anion exchange chromatography), we were able to isolate different enzyme pools: four partially purified β-xylosidase/arabinofuranoside; *FpXylEAB* trifunctional GH10 *endo*-xylanase/β-xylosidase/arabinofuranoside enzyme (39.8 kDa) and *FpXynE* GH11 endo-xylanase with molecular mass (18.0 kDa). *FpXylEAB* and *FpXynE* enzymes were highly active at pH 5–6 and 60–50 °C.

1. Introduction

Prebiotics are non-digestible food ingredients that can promote the growth of beneficial gut microbiota. For instance, xylooligosaccharides (XOS) from 2 to 4 xylose units (X_2-X_4) can be selectively used by *Bifidobacterium* spp. [1].

XOS can be obtained from lignocellulosic biomass by enzymatic hydrolysis of the hemicellulose fraction (xylan) using xylanolytic enzymes [2]. However, the most common product released from that enzymatic hydrolysis comprises XOS mixture with variable sizes (only 10–60 % of the total hydrolysed xylan is X_2-X_4) [3]. Thus, to maximise the X_2-X_4 content, it is necessary to find enzymes able to act or shorter XOS (XOS > X_5). In this sense, β-xylosidases might be the preferable enzymes [4], although some *endo*-xylanases may be able to act on those products too [5].

Several fungal species can decompose and modify natural biomass by secreting and expelling diverse carbohydrate-active enzymes [6]. Particularly, the genome of *Fusarium* species encodes numerous lignocellulosic enzymes, showing a higher content of β-xylosidase and *endo*-xylanases in contrast with other fungi species [7]. However, *Fusarium*

Abbreviations: CV, column volumes; DNS, 3,5-dinitrosalicylic acid; DP, degree of polymerisation; GH, glycoside hydrolase; MM, molecular mass; MUM, Micoteca da Universidade do Minho; MUX, 4-methylumbelliferyl-β-D-xylopyranoside; PDA, potato dextrose agar; pNP, *p*-nitrophenol; pNP-A, *p*-nitrophenyl α-L-arabinofuranoside; pNP-X, *p*-nitrophenyl β-Dxylopyranoside; RT, room temperature; X_2, xylobiose; X_4, xylotetraose; XOS, xylooligosaccharides.

* Corresponding author.
E-mail address: mlrua@uvigo.es (M.L. Rúa).

https://doi.org/10.1016/j.ijbiomac.2024.132722
Received 22 December 2023; Received in revised form 23 May 2024; Accepted 27 May 2024
Available online 29 May 2024

xylanolytic enzyme production potential has not been explored enough: among the 700 species belonging to *Fusarium* genera, *F. oxysporum* and *F. graminearum* have been the xylanase-producers mostly studied [8].

When extracellular enzymes are isolated, compounds commonly released by fungi, such as polyphenols, pigments, polysaccharides (including those incorporated into the culture media as inductors), proteases, and other small molecules, may greatly interfere with the purification procedures [9–12].

To separate these contaminants from the proteins of interest, most common purification protocols include an initial clarification step through ultrafiltration, size exclusion chromatography, or bulk precipitation methodologies. Then, the partially purified enzymes are selectively separated using different chromatographic steps [13–16]. However, clarification techniques are not always fully effective in eliminating some of those contaminants (particularly polymeric compounds). Depending on the membrane cut-off, polymers could be retained in the ultrafiltration process together with the proteins. Also, carbohydrates precipitate when ethanol or ammonium sulfate are used and can be recovered in the pellet obtained after precipitation, together with the proteins of interest. Besides, considering that precipitation methods are not only a purification step but also a concentration step, these polysaccharides are concentrated, increasing the density of the solution which maximises the issues prior to chromatographic steps. This complexity may lay behind the often very low reported yields (2.6–20 %) for the recovery of xylanases and other fungal enzymes [11,15,17,18]. A recalcitrant association of the enzyme with components from the culture media, in many cases coloured, have been previously reported [19].

Thus, the present research aimed to assess the production of xylanolytic enzymes from *Fusarium pernambucanum* MUM 18.62 strain, comparing its enzyme expression with several *Fusarium* species and other crop pathogen fungi. Additionally, xylanolytic enzyme expression was optimised by determining the influence of the carbon source in the pre-inoculum. A method to eliminate compounds that interfere with the purification is detailed as well as the optimised sequential purification of extracellular β-xylosidases, arabinofuranosidases, and *endo*-xylanases enzymes. Proteins obtained in the different purified extract were identified by peptide-mass fingerprinting, and purest extracts were characterised in terms of optimal pH and temperature for their activity, as well as their stability. To our knowledge, this is the first report on the purification, identification and characterisation of xylanolytic enzymes from the species *F. pernambucanum* MUM 18.62.

2. Materials and methods

2.1. Materials

Fungi strains (*Fusarium graminearum* MUM 17.22, *Fusarium redolens* MUM 20.75, *Fusarium pernambucanum* MUM 18.62, *Fusarium caatingaense* MUM 18.59, *Chaetomium globosum* MUM 18.08, *Alternaria alternata* MUM 16.02, *Alternaria atra* MUM 9712, *Stachybotrys chartarum* MUM 19.88, *Ganoderma applanatum* MUM 04.103) were kindly supplied by Micoteca da Universidade do Minho (MUM) (Braga, Portugal).

Xylan from beechwood and xylan from corncob with >95 % XOS were purchased from Carl Roth (Karlsruhe, Germany). Arabinoxylan was purchased from Megazyme (Wicklow, Ireland). *p*-Nitrophenyl β-D-xylopyranoside (pNP-X), *p*-nitrophenylα-L-arabinofuranoside (pNP-A), and 4-methylumbelliferyl-β-D-xylopyranoside (MUX) were acquired from Sigma (St Louis, MO, USA).

Fungal strains were grown on Potato dextrose agar (PDA, Oxoid CM0139) and on xylan-enriched Czapek agar (% *w/v*): 1.5 % xylan from corncob; 1.5 % xylan from beechwood; 1.5 agar; 0.5 % yeast extract; 0.1 % K_2HPO_4 and 1 % Czapek concentrate (30 % $NaNO_3$; 5 % KCl; 5 % $MgSO_4.7H_2O$; 0.1 % $FeSO_4.7H_2O$; 1 % $ZnSO_4.7H_2O$; 0.5 % $CuSO_4.5H_2O$). Liquid cultures consisted on xylan-enriched Czapek media without agar.

All other chemicals were of the purest grade available.

2.2. β-Xylosidase screening

All fungal strains supplied by MUM were grown on PDA at 30 °C, in the dark. After 7 days, 100 mL of Czapek liquid media, enriched with 1.5 % xylan from corncob and 1.5 % xylan from beechwood (xylan-enriched Czapek), was inoculated with mycelial agar plugs of 5 mm diameter. Flaks were incubated for 11 days at 26 ± 1 °C with shaking at 120 rpm.

β-xylosidase production was followed daily by measuring enzymatic activity at 30 °C and two pH values (5.5 and 8), following the methodology described in Section 2.6.1.

2.3. Fungi selection and culture conditions for enzyme production

F. pernambucanum MUM 18.62 was grown in both, PDA and xylan-enriched Czapek agar for 7 days at 30 °C.

After 7 days, flasks with xylan-enriched Czapek liquid media were inoculated with a plug from both agar plates as explained in Section 2.2. Flasks were incubated for 8 days at 30 °C with shaking at 120 rpm. Aliquots of 2 mL were taken daily. At the end fungal cells were removed from the culture broth first by filtration through filter paper and second by centrifugation (30.100 ×*g* for 30 min). The clarified supernatant was used as the source of crude enzyme.

β-Xylosidase and *endo*-xylanase activities were determined at 30 °C and pH 8, following the protocol described in Section 2.6. pH variation was also followed.

Cell growth was estimated by the sugar consumption using the phenol-sulfuric acid method [20]. Briefly, 0.25 mL diluted culture media were mixed with 0.25 mL of phenol solution (50 g L^{-1}). Then, 1.25 mL of hydrazine sulfate solution at 5 g L^{-1} prepared in concentrated sulfuric acid was added rapidly to the mixture and well mixed. Samples were cooled down at room temperature. Light absorption at 490 nm was measured in a microplate scanning spectrophotometer FLUOstar Omega (BMG Labtech, Offenburg, Germany). Xylose standard curve from 0 to 0.1 g L^{-1} was used for xylose quantification.

Statistical analysis was performed with GraphPad Prism 8.0.2 software (GraphPad Software Inc.). The student's *t*-test was used to analyse the differences between the pre-inoculum source in regard to the cell growth and enzyme production.

2.4. Purification

2.4.1. Ammonium sulfate precipitation (ASP)

F. pernambucanum MUM 18.62 extracellular media obtained after 8 days of culture (EC0) was precipitated by adding solid $(NH_4)_2SO_4$ until 50 % (*w/v*) ammonium sulfate saturation (final concentration: 2.2 M). The solution was kept stirring for 1 h in an ice bath after the full addition. The supernatant was recovered after centrifugation (30.100 ×*g* for 30 min) and diluted 1.3-fold with 50 mM sodium phosphate buffer pH 6.8 to obtain a 1.7 M ammonium sulfate solution (ASP_EC1) to be loaded on hydrophobic columns (Fig. 1).

2.4.2. Hydrophobic interaction chromatography

2.4.2.1. Hydrophobic interaction chromatography 1 (HIC1). The crude extract ASP_EC1 from ASP (Fig. 1) was loaded at 1.2 mL min^{-1} flow rate on a handmade Phenyl Sepharose 6FF (low sub) (9.2 × 2.6 cm) column (volume: 50 mL, GE Healthcare, Sweden) coupled to an ÄKTA Purifier 10 (GE Healthcare Bio-Sciences AB, Uppsala, Sweden) following the instructions provided by the manufacturer. The column was equilibrated with 50 mM sodium phosphate buffer pH 6.8 at room temperature (RT), containing 1.7 M $(NH_4)_2SO_4$. Elution was performed at 1.5 mL min^{-1} flow rate with 20 column volumes (CV) linear gradient from

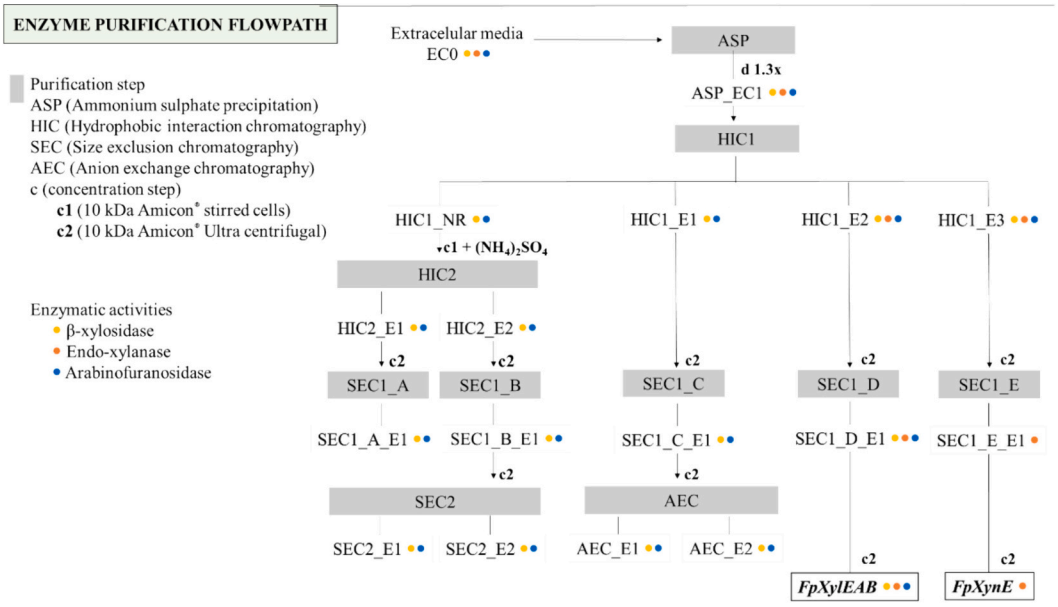

Fig. 1. Summary of the purification process of the different enzymatic extracts obtained from *F. pernambucanum* MUM 18.62 extracellular media.

equilibration buffer to 50 mM phosphate buffer pH 6.8 at 25 °C (buffer B). Fractions of 5 mL were collected.

2.4.2.2. Hydrophobic interaction chromatography 2 (HIC2). Non-retained fraction (HIC1_NR) (Fig. 1) from HIC1 was concentrated to 500 mL using an Amicon® stirred cell (Millipore, CA, USA) through a 10 kDa molecular weight cut-off (MWCO) membrane. Solid $(NH_4)_2SO_4$ was added to the permeated fraction up to final concentration of 2.2 M. Sample was centrifuged (30.100 ×*g* for 30 min) and supernatant was re-loaded at 1.2 mL min^{-1} on the Phenyl Sepharose column coupled to the ÄKTA Purifier 10, equilibrated with 50 mM phosphate buffer pH 6.8 at 25 °C with 2.2 M $(NH_4)_2SO_4$. Elution was performed at 1.2 mL min^{-1} flow rate decreasing the $(NH_4)_2SO_4$ concentration with 50 mM phosphate buffer pH 6.8 at 25 °C (buffer B), in three steps: (1) 5 CV with 25 % buffer B, (2) 5 CV with 55 % buffer B, and (3) 5 CV with 100 % buffer B. Fractions of 10 mL were collected.

Those fractions from previous chromatographic steps in which β-xylosidase, *endo*-xylanase and arabinofuranosidase activities were detected, were pooled following the chromatographic profile, obtaining the fractions: HIC1_E1, HIC1_E2, and HIC1_E3 from HIC1; and HIC2_E1 and HIC2_E2 from HIC2. Finally, they were concentrated using Amicon® Ultra centrifugal tubes with 10 kDa MWCO and stored at −40 °C for next purification steps.

2.4.3. Size exclusion chromatography

2.4.3.1. Size exclusion chromatography (SEC1). The pooled fractions from HIC1 (HIC1_E1, HIC1_E2 and HIC1_E3) and HIC2 (HIC2_E1 and HIC2_E2) (Fig. 1) were loaded onto a HiLoad® 16/60 Superdex® 75 prep grade SEC column (volume: 120 mL, GE Healthcare, Sweden) coupled to the ÄKTA Purifier 10. SEC column was equilibrated with 20 mM sodium phosphate buffer pH 7.0 with 150 mM NaCl and 0.05 % (*w/v*) sodium azide. Elution was performed at 0.3 mL min^{-1} and fractions of 0.5 mL were collected. Fractions active for β-xylosidase, *endo*-xylanase and arabinofuranosidase activities were pooled according with the chromatogram, obtaining the following fractions: SEC1_A_E1 from SEC1_A; SEC1_B_E1 from SEC1_B; SEC1_C_E1 from SEC1_C; SEC1_D_E1 from SEC1_D; and SEC1_E_E1 from SEC1_E (Fig. 1). SEC1_B_E1 fraction was concentrated using Amicon® Ultra centrifugal tubes with 10 kDa MWCO and stored at −40 °C for the next purification steps. SEC1_C_E1 was also concentrated and included in new purification steps. The other fractions were stored at −40 °C.

2.4.3.2. Size exclusion chromatography (SEC2). The active fraction SEC1_B_E1 from SEC1_B (Fig. 1) was loaded onto a HiPrep™ 16/60 Sephacryl® S-200 SEC column (volume: 120 mL, Pharmacia Biotech) coupled to the ÄKTA Purifier 10. The column was equilibrated in the same buffer as the *SEC1* chromatography. Elution was performed at 0.3 mL min^{-1} and fractions of 0.5 mL were collected. Fractions active for β-xylosidase, *endo*-xylanase, and arabinofuranosidase activities were pooled following the chromatogram, and stored at −40 °C for characterisation and identification. The obtained fractions were: SEC2_E1 and SEC2_E2 (Fig. 1).

2.4.4. Anion exchange chromatography (AEC)

SEC1_C_E1 concentrated fraction, obtained from the SEC1_C step (Fig. 1), was run on PD-10 desalting columns (Pharmacia Biotech, NJ, USA) to equilibrate them in 20 mM Piperazine-HCl buffer pH 5 (equilibration buffer). Then, samples were loaded on an equilibrated MonoQ 5/50 GL column (volume: 1 mL, Cytiva, MA, USA) column at 0.8 mL min^{-1}. Elution was performed at 1 mL min^{-1} flow rate with a 40 CV linear gradient from equilibration buffer to the same containing 1 M NaCl. Those fractions active for β-xylosidase, *endo*-xylanase and arabinofuranosidase activities were pooled and stored at −40 °C. Two pools were obtained: AEC_E1 and AEC_E2 (Fig. 1).

2.5. Electrophoresis and zymogram analysis

Enzymatic extracts obtained after each purification step (except final pools, which were analysed according to Section 2.8) were analysed by sodium dodecyl sulfate-polyacrylamide gel electrophoresis (SDS-PAGE). Electrophoresis was performed with 10–12 % acrylamide separating gel and 4 % acrylamide stacking gel in a Mini Gel Tank at 225 V following manufacturer's specifications. Samples were mixed with loading buffer (% (*w/v*) SDS and 2 % (v/v) 2-mercaptoethanol), boiled for 5 min and loaded onto the gel. Protein bands were visualised by Coomassie Brilliant Blue R-250 staining according to standard procedures. Precision plus protein unstained standards (10–250 kDa) (Biorad, Richmond, CA, USA) were used as standards.

Zymogram analysis for *endo*-xylanase activity was done according to Rodríguez-Sanz et al. [2] in a SE260 Mini Vertical Protein Electrophoresis unit (Hoefer Inc., Holliston, USA) under refrigeration.

Electrophoresis was performed in 10 % (v/v) polyacrylamide gels including 0.5 % (*w/v*) arabinoxylan, with 4 % stacking gel. *FpXylEAB* and *FpXynE* were mixed with loading buffer with SDS and 2-mercaptoethanol, boiled for 2 min and loaded onto the gel. After electrophoresis, enzymes were refolded by washing the gel with 2.5 % (v/v) Triton X-100 in 25 mM citrate-phosphate buffer (pH 6.0) for 30 min at RT.

2.6. Enzyme activity assays

Measurements were made for triplicate in microplate scanning spectrophotometer FLUOstar Omega (BMG Labtech, Offenburg, Germany).

2.6.1. β-Xylosidase and arabinofuranosidase activity

An aliquot of 100 μL of 25 mM *p*-nitrophenyl xylopyranoside (pNP-X) or *p*-nitrophenyl α-L-arabinofuranoside (pNP-A) were mixed with 800 μL of 25 mM sodium phosphate buffer pH 8.0, and 100 μL of appropriately diluted enzymatic solution. Incubation was made at 30 °C for 20 min. Reaction was stopped by adding 250 μL 1 M Na_2CO_3 and cooling down on ice for 5 min. Then samples were incubated 5 min at room temperature and absorbance was measured at 400 nm.

A *p*-nitrophenol standard curve from 0 to 50 μM was used for pNP quantification. The standard mixture contained 100 μL of each pNP standard, 800 μL buffer, 100 μL distilled water, and 250 μL of 1 M sodium carbonate. One unit of β-xylosidase and arabinofuranosidase activity was defined as the amount of enzyme that produced 1 μmol of pNP per minute.

2.6.2. Endo-xylanase activity

An aliquot of 180 μL 1 % (*w/v*) arabinoxylan was incubated for 20 min at 30 °C with 20 μL diluted enzymatic solution. At the end of the incubation time, 300 μL of 3,5-dinitrosalicylic acid (DNS) were added to stop the enzymatic reaction. Samples were boiled 5 min, cooled down on ice for 5 min, and measured after 5 min at room temperature. Quantification was made at 540 nm [21].

A xylose standard curve was built from 0 to 0.5 g L^{-1} for xylose quantification. Substrate and diluted enzyme were replaced by 180 μL of xylose standard, and 20 μL water, respectively. One unit of *endo*-xylanase activity was defined as the amount of enzyme that produced 1 μmol of xylose per minute.

2.7. Protein quantification

2.7.1. BCA

Protein concentrations of all crude extracts included in the different purification steps were measured by Pierce BCA Protein Assay Kit (Pierce, Rockford, IL) with bovine serum albumin (BSA) as the standard.

2.7.2. Nanodrop

Protein concentration in the purified extracts (SEC2_E1, SEC2_E2, SEC1_D_E1 (named as *FpXylEAB*) and SEC1_E_E1 (named as *FpXynE*) were checked by spectrophotometry at 280 nm on a Thermo Scientific NanoDrop 2000c (Wilmington, DE, USA).

2.8. Peptide-mass fingerprinting analysis

SEC2_E1, SEC2_E2, AEC_E1, AEC_E2, SEC1_D_E1 (*FpXylEAB)* and SEC_E_E1 (*FpXynE)* samples (Fig. 1) were analysed by sodium dodecyl sulfate (SDS)-polyacrylamide gel electrophoresis (PAGE) using a precast Novex™ 10–20 % Tricine gel (Invitrogen, Wilmington, DE, USA) in a Mini Gel Tank, following the manufactures' protocol. Samples were mixed 1:1 (v/v) with Novex Tricine SDS Sample Buffer (2×) with 2 % (v/v) 2-mercaptoethanol and heated at 85 °C for 2 min. After electrophoresis, gel was stained with Colloidal Coomassie for bands visualisation following standard procedures.

Visualised bands were cut and gel pieces were subjected to in-gel digestion with trypsin. The obtained peptides were loaded onto a reverse phase column (PepMap® RSLC C18, 2 μm, 100 Å, 75 μm × 50 cm, Thermo Fisher Scientific) and eluted in a linear gradient from 5 to 35 % acetonitrile containing 0.1 % formic acid for 240 min at 0.3 mL min^{-1}. Eluted peptides were analysed by electrospray ionization-tandem mass spectrometry on a hybrid high-resolution LTQ-Orbitrap Elite mass spectrometer coupled to a Proxeon Easy-nLC 1000 UHPLC system (ThermoFisher Scientific) (CACTI, University of Vigo, Spain).

For Peptide Mass Fingerprint analysis, the MASCOT and PEAKS search engines were used. Peptide fingerprint was constructed matching the obtained peptides with SwissProt reviewed proteins and TrEMBL unreviewed proteins. SwissProt searching was made against Fungi proteins (taxon ID 4761) whereas TrEMBL searching was limited to *Fusarium* genera (taxon ID 5506).

2.9. Biochemical characterisation of extracellular xylanolytic enzymes

2.9.1. Optimal pH and temperature

Optimal pH and temperature for activity were determined for *Fusarium pernambucanum* MUM 18.62 pure enzymes: SEC1_D_E1, SEC1_E_E1 (renamed as *FpXylEBA* and *FpXynE*, respectively). The effect of the pH was determined from 4.0 to 10.0 at 30 °C. Buffers used were: 25 mM citrate-phosphate buffer (pH 5 and 6), 25 mM sodium phosphate buffer (pH 7 and 8) and 25 mM sodium carbonate buffer (pH 9 and 10). pH of the buffer solutions was adjusted at 30 °C. The effect of temperature was determined from 20 °C to 80 °C at the optimal pH for each enzyme. The pH of buffer solutions was adjusted at each assayed temperature.

Endo-xylanase activity optimum condition was measured according to Section 2.6.2 with arabinoxylan as substrate. β-Xylosidase and arabinofuranosidase activity were measured with pNP-X and pNP-X substrates (Section 2.6.1).

2.9.2. Stability

Thermal inactivation of the pure enzymes *FpXylEBA* and *FpXynE* was studied at 60 and 50 °C, respectively. Pure enzymes were diluted 5-fold in 25 mM citrate-phosphate buffer pH 6 and incubated for 24 h in a thermostatic water bath (MultiTempII, GE Healthcare, Sweden). At regular incubation times (0, 1, 2, 4, 6, 12 and 24 h), aliquots were withdrawn, cooled down and centrifuged for the measurement of residual activity. Endo-xylanase activity was quantified according to Section 2.6.2 at optimal conditions.

Operational stability was studied at 60 °C for *FpXylEBA* and 50 °C for *FpXynE* in presence of substrate. Pure enzymes were diluted 10-fold in 25 mM citrate-phosphate buffer pH 6 with 1 % (w/v) arabinoxylan (final volume 200 μL) and incubated for 1 h in a thermobloc (ThermoMixer C, Eppendorf, Germany). At regular incubation times (0, 5, 10, 20, 30, 40, and 60 min), reaction was stopped with 300 μL 3,5-dinitrosalicylic acid (DNS). Samples were boiled 5 min, cooled down on ice for 5 min, and absorbance was measured after 5 min at room temperature. Quantification was made at 540 nm [21].

Weibull equation is a classical sigmoidal equation [22] that has been previously described as useful for modelling experimental data of enzyme hydrolysis Eq. [23]. So, product generation was fitted to this equation with GraphPad Prism 8.0.2 (GraphPad Software Inc., San Diego, CA, U.S.A.) to evaluate operational stability and/or substrate/product inhibition:

$$H = H_m\left\{1 - exp\left[-LN2\left(\frac{t}{\tau}\right)^{\beta}\right]\right\} \quad (1)$$

where H is the percentage of initial product which was hydrolysed (%), and t is the time of hydrolysis (min). H_m is the maximum degree of hydrolysis (%), β is a dimensionless parameter related to the maximum slope of hydrolysis, τ is the time required to achieve the semi-maximum degree of hydrolysis (min). From the values of these parameters, v_m, the maximum hydrolysis rate at the τ-time (% min^{-1}), and t_m, time required

to achieve the beginning of asymptote phase (H_m) (min), were calculated as follows [22]:

$$v_m = \frac{H_m \bullet \beta \bullet LN2}{2 \bullet \tau} \quad (2)$$

$$t_m = \tau\left(\frac{\beta - 1}{\beta \bullet LN2}\right)^{1/\beta} + \frac{H_m}{2 \bullet v_m} \quad (3)$$

3. Results and discussion

3.1. Screening of β-xylosidase fungi producers

Different fungi species were selected from the culture collection of the Micoteca da Universidade do Minho (MUM) to be evaluated for β-xylosidase enzyme production (Table 1): *Fusarium graminearum* MUM 17.22, *Fusarium redolens* MUM 20.75, *Fusarium pernambucanum* MUM 18.62, *Fusarium caatingaense* MUM 18.59, *Chaetomium globosum* MUM 18.08, *Alternaria alternata* MUM 16.02, *Alternaria atra* MUM 9712, *Stachybotrys chartarum* MUM 19.88 and *Ganoderma applanatum* MUM 04.103.

Fungi belonging to *Fusarium* species have been broadly studied as source of different lignocellulosic enzymes since they are able to infect many different crop species [8]. Among the selected *Fusarium* species to be evaluated from MUM culture collection, *Fusarium graminearum* has been the most thoroughly studied with many xylanolytic enzymes already known [11,24,25], and with other many xylanolytic genes already identified in its genome [26]. However, *F. redolens*, *F. pernambucanum* and *F. caatingaense* have not been previously identified as xylanolytic enzymes producers.

On the other hand, *Chaetomium globosum* and *Alternaria alternata* fungi species have been previously recognized as producers of cellulolytic and xylanolytic enzymes with low hydrolysis rates. However, they can degrade wood under extreme environmental conditions [27], being a promising source of enzymes with high stability. *Alternaria* fungal genus has been associated with different plant diseases [28], therefore *Alternaria atra* was also included in the β-xylosidase screening.

Ganoderma applanatum and *Stachybotrys chartarum*, are reported to have a lignocellulose complex-degrading enzyme system with mannanases, glucanases, and xylanases, among other enzymes [29,30]. Nevertheless, β-xylosidases have not been described for those fungi.

Although most of the selected fungi species have been described as xylanolytic enzymes producers, β-xylosidases have not been identified in many of them. Thus, the ability of these fungi species to produce β-xylosidases, and most critically, those able to work at alkaline pH were targeted in this work (Table 1). To that end, the selected fungi were grown in Czapek liquid media enriched with xylan from beechwood and corn cob as carbon sources. Particularly, β-xylosidase production was expected to be induced by corn cob as, according to our own analysis, 53 % of the oligomers in this xylan are oligomers with 2 to 4 xylose units (X_2-X_4) whereas 38 % are polymers with >11 xylose units (X_{11}). On the contrary, X_{11} represent 99.5 % of the xylan contained in beechwood xylan.

All the evaluated species were positive for β-xylosidase activity at the assayed conditions (pH 5.5 and 8) (Table 1). Species belonging to *Fusarium* genera were among the most active, although *F. graminearum* MUM 17.22 showed the lowest β-xylosidase activity of all the evaluated species (Table 1). These results were unexpected considering that *endo*-xylanases from *F. graminearum* are described as highly active and highly stable at 30–40 °C [25,31], and we foresaw similar optimum working conditions for its β-xylosidases.

The highest β-xylosidase was detected for *F. pernambucanum* MUM 18.62 with 32.8 × 10^{-3} U mL^{-1} at pH 8, and *F. caatingaense* MUM 18.59 with 29.6 × 10^{-3} U mL^{-1} at pH 5.5. They had 13.6 to 25-fold higher β-xylosidase activity than *F. graminearum*. Regarding *F. redolens* MUM 20.75, it showed intermediate activity among all the species evaluated, with the highest values at pH 5.5, i.e. 3-fold lower than the β-xylosidase activity showed by *F. pernambucanum*, but 4.6-fold higher than that one showed by *F. graminearum*.

Among the other genera, *C. globosum* MUM 18.08 and *A. alternate* MUM 16.02 were positioned in 3rd and 4th place with just 1.4 to 2-fold less β-xylosidase activity than *F. pernambucanum*. However, these species showed the highest difference between activities at pH 5.5 and 8, being between 1.5 and 5.7-fold more active at pH 8. In relation to *S. chartarum* MUM 19.88, *A. atra* MUM 97.12 and *G. applanatum* MUM 04.103, all of them showed at least 3-fold less β-xylosidase activity than the most active one, *F. pernambucanum* (Table 1).

Taking into consideration that this strain of *F. pernambucanum* showed the highest β-xylosidase activity among all the evaluated species; its activity was higher at alkaline than at acid pH; and the maximum β-xylosidase activity was reached at a short culture time (Table 1); it was chosen for the optimisation of culture conditions, purification, and characterisation of its relevant enzymes. On the other hand, all the evaluated species are now recognized as β-xylosidase producers, and future research will be devoted to their study.

Table 1
β-Xylosidase activity determined in the extracellular media of different fungi belonging to MUM culture collection.

Fungi species	Collection n°[a]	β-Xylosidase activity (10^{-3} U mL^{-1})[b]		
		pH 5.5	**pH 8**	Day[c]
1. *Fusarium pernambucanum*	**MUM 18.62**	25.9	**32.8**	7
2. *Fusarium caatingaense*	MUM 18.59	29.6	**29.4**	7
3. *Chaetomium globosum*	MUM 18.08	15.2	**22.9**	10
4. *Alternaria alternata*	MUM 16.02	5.9	**16.6**	7
5. *Fusarium redolens*	MUM 20.75	8.8	**7.8**	10
6. *Stachybotrys chartarum*	MUM 19.88	6.3	**7.8**	11
7. *Alternaria atra*	MUM 97.12	7.9	**7.1**	11
8. *Ganoderma applanatum*	MUM 04.103	2.2	**1.5**	5
9. *Fusarium graminearum*	MUM 17.22	1.9	**1.3**	11

[a] Numbering of the culture collection of the Micoteca da Universidade do Minho (MUM), Braga, Portugal.
[b] β-xylosidase activity was determined using 2.5 mM pNP-X for 20 min at 30 °C.
[c] Day when maximum β-xylosidase activity was detected for each fungal strain. Fungi were cultured at 26 ± 1 °C and 120 rpm in liquid Czapek media enriched with 1.5 % corncob xylan and 1.5 % beechwood xylan.

3.2. Optimisation of Fusarium pernambucanum MUM 18.62 xylanolytic enzymes production

When fungi are grown in liquid media, inoculum usually comes from plugs of the fungi previously incubated in common agar plates (e.g., PDA plates), and culture optimisation usually relays in liquid media composition [29,32–34]. However, adaptation time may vary when different carbon sources are employed in the different solid/liquid media, likely influencing enzyme production (in this case, xylanolytic enzyme expression). Therefore, in this work, *F. pernambucanum* β-xylosidase production was evaluated considering the inoculum origin which has also been regarded as influential [35]. For these studies, levels of *endo*-xylanase activity were also studied.

F. pernambucanum pre-inoculum was grown in PDA plates and xylan-enriched Czapek agar plates (with xylan as the main carbon source). After 7 days at 30 °C, mycelial agar plugs of each plate were used as inoculum in Czapek liquid media with xylan (1 plug for each 100 mL media). Flasks were incubated for 8 days at 30 °C under continuous shaking (Section 2.3), and aliquots were taken daily to follow fungal growth and enzyme production. Three independent flasks were made for each pre-inoculum source ($n = 3$).

Cell growth was followed by total sugar consumption (Fig. 2A) and pH variation in the culture media (Fig. 2B). At the same time, extracellular media was screened for β-xylosidase (Fig. 2C, above) and *endo*-

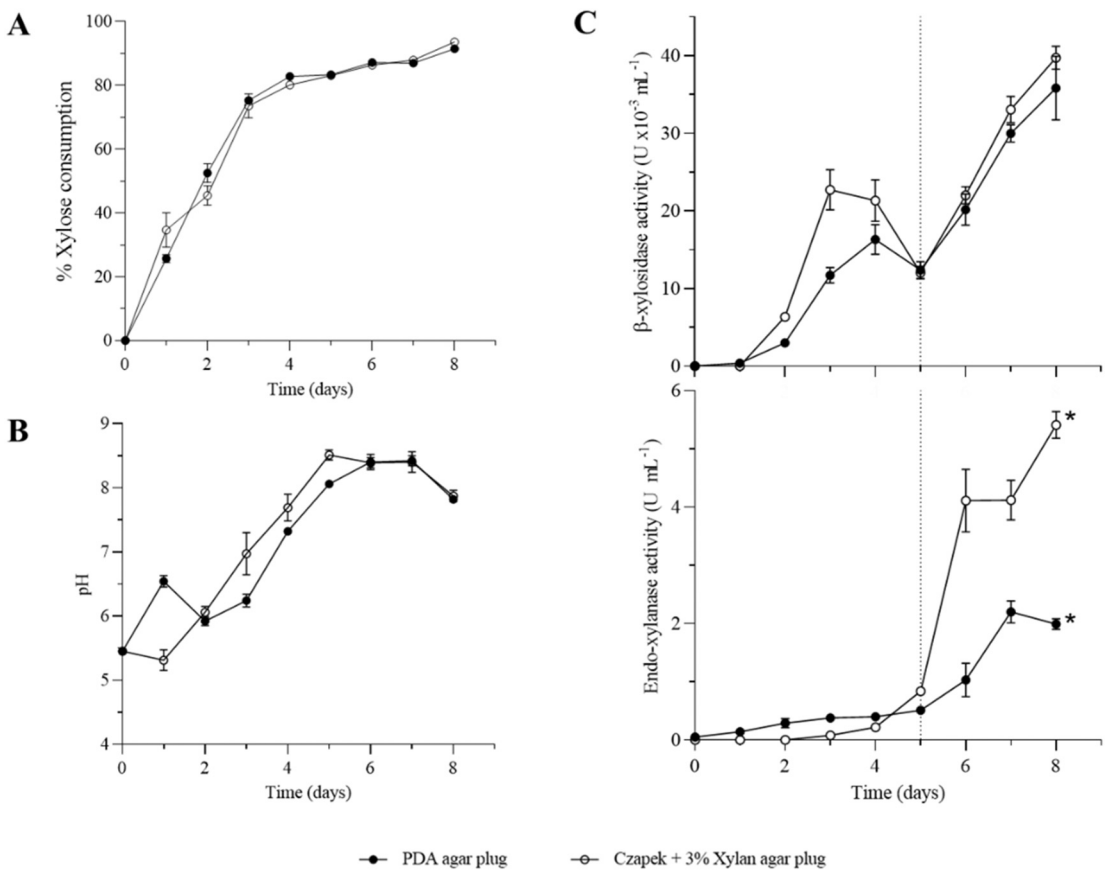

Fig. 2. Evolution of *Fusarium pernambucanum* MUM 18.62 culture at 30 °C in Czapek liquid media with 3 % xylan after inoculum with plugs from PDA (●) or xylan-enriched Czapek agar (○) plates. (A) Total sugar consumption. (B) pH media variation. (C) β-xylosidase and *endo*-xylanase production. * Significant differences ($p < 0.05$).

xylanase (Fig. 2C, below) activities using pNP-X and DNS method, respectively, as explained in Section 2.3.

Total sugar consumption and pH media evolved similarly irrespective of the inoculum source (Fig. 2A). Both cultures consumed >90 % of the total sugar content, being slightly lower (but not significantly different, $p > 0,05$) with the PDA inoculum (91.4 ± 0.3 %) than Czapek agar plates inoculum (93.6 ± 1.0 %). Regarding the pH variation, both cultures started with pH 5.5, but achieved the maximum pH at different days (5 days with Czapek agar and 7 days with PDA, respectively), with values around pH 8.5. However, at the end of the assay (day 8), pH decreased in both cultures to pH 7.8 (Fig. 2B).

The xylanolytic system in filamentous fungi responds to induction and repression [36,37]. Najjarzadeh et al. [38] have demonstrated that xylooligosaccharides are more effective than other substrates at inducing *endo*-xylanase and β-xylosidases from *Fusarium oxysporum f.* sp. *Lycopersici*, reporting a correlation between the xylooligosaccharide degree of polymerisation (DP) and induction efficiency of each enzyme.

In our experiment, levels of endo-xylanase were at minimum or null for almost 5 days, but after day 1, β-xylosidase activity was already noticeable and increased up to a maximum after 3–4 days, depending on the agar plug used as inoculum. Levels of β-xylosidase reached higher numbers for the case of cultures inoculated with Czapek agar plugs (Fig. 2C, above). These results suggested that during this 5-days period the studied strain was growing at the expenses of sugars derived from small DP-xylan oligomers hydrolysed by the inducible β-xylosidase secreted to the media. Precisely, as indicated above, the content of these xylan oligosaccharides was relevant in the culture media which included a 1:1 mixture of corn cob (53 % are X_2-X_4) and beechwood xylan (95 % are $>X_{11}$).

As indicated, *endo*-xylanase activity was extremely low until day 5 when it peaked up matching with the decay of β-xylosidase activity after the first maxima. It is interesting that between days 4 and 5, consumption of xylose also slowed down after an almost linear increase from 0 to 80 %, and pH stabilises at 8.5, strongly suggesting that a physiological change was occurring at this time. As long DP-xylan might be by now the only substrates at disposal for the strain, growth was likely dependent on their hydrolysis into small DP-XOS. To that end more extracellular *endo*-xylanase was required in the medium, explaining the increase in its production in parallel with the second round of β-xylosidase activity increase, an enzyme that is known to act synergistically with the endo-enzyme [39,40].

The endo-xylanase activity was clearly favored in cultures with the inoculum from the xylan-enriched Czapek agar plates with 5.4 ± 0.2 U mL^{-1} maximum activity after 8 days of culture. The maximum endo-xylanase activity inoculated from the PDA plates was 2.2 ± 0.2 U mL^{-1} (2.5 folds lower) after 7 days' cultivation.

In this work, higher productions of initial β-xylosidase (up to day 5) and *endo*-xylanase were reached using the pre-inoculum growth in the same complex carbon source (in our case, Czapek agar plates enriched with xylan). Sequential growth of several fungi (ex. *Pleurotus ostreatus*, *Aspergillus niger* or several *Trichoderma* strains) in which a submerged fermentation is preceded by a solid-state pre-culture step with the inducer substrate has been reported to increase the expression of some hydrolytic enzymes growing on lignocellulosic biomass [35,41–43].

This higher expression might be related to the inductor effect of xylan during the early stages of fungal development. Xylan could, in some way, enhance the induction-expression mechanisms in the inoculum generating a more efficient fungal biomass to produce the enzymes when they are needed during the culture.

3.3. Xylanolytic enzymes purification

Extracellular culture obtained after 8 days of growing *F. pernambucanum* MUM 18.62 in xylan-enriched Czapek liquid media inoculated with xylan-enriched Czapek agar plugs was used as crude extract for protein purification (EC0, Fig. 1). Focus was kept on β-xylosidase and endo-xylanase activities together with the analysis of arabinofuranosidase, as several xylanolityc enzymes having dual activity (β-xylosidase/arabinofuranosidase) have been described in the literature [4].

Purification steps faced difficulties due to EC0 composition; a brown and dense extract obtained after the culture centrifugation. When EC0 was directly loaded onto chromatographic adsorption resins (anionic and cationic exchange chromatography), no reproducible chromatograms were obtained (protein elution was not dependent on the percent of eluent -ionic strength-, but on the volume of the loaded crude extract). Thus, the removal of the interferences was the first aim for proper enzyme purification.

Ethanol was the first attempt to precipitate proteins keeping the dense material soluble. However, it resulted in a clear supernatant negative for xylanolytic activities, and a brown dense precipitate positive for xylanolytic activities, likely associated to polymeric substances (possibly polysaccharides) in EC0 that precipitate with organic compounds. These might come from exopolymeric substances produced by *Fusarium* species [9,10], and/or the 6.4–8.6 % residual xylan that was not consumed during growth (Fig. 2A). Besides, only 20 % of the initial β-xylosidase remained active in the precipitate (data not shown). Same results were obtained with other organic solvents such as acetone.

Ammonium sulfate salt was alternatively evaluated as bulk precipitation step (ASP). Thus, EC0 was precipitated with 50 % saturated ammonium sulfate salt for 1 h on an ice bath, as it is described in Section 2.4.1. This treatment triggered the precipitation of dense compounds while 90 % β-xylosidase, 42 % *endo*-xylanase, and 80 % arabinofuranosidase activities were kept in the supernatant. Likewise, the ASP step (Fig. 1) precipitated contaminant proteins, and hence increased purification factors to 4.7 for β-xylosidase, 2.2 for endo-xylanase, and 4.2 for arabinofuranosidase (Table 2).

3.3.1. Hydrophobic interaction chromatography (HIC1)

Contrary to most common purification protocols where targeted enzymes are recovered in the pellet [44,45], our purification protocol started with the supernatant obtained after ammonium sulfate precipitation. This supernatant was diluted 1.3× to decrease ammonium sulfate content from 2.2 M (≈50 % saturation) to 1.7 M (APS_EC1, Fig. 1). APS_EC1 was loaded then onto a handmade Phenyl Sepharose™ 6 FF column and eluted following the methodology described in Section 2.4.2 (HIC1).

Four active fractions were obtained, from low to high hydrophobicity (Fig. 3): non-retained fraction (HIC1_NR), eluted fraction 1 (HIC1_E1), eluted fraction 2 (HIC1_E2), and eluted fraction 3 (HIC1_E3). HIC1_NR and HIC1_E1 were positive for β-xylosidase and arabinofuranosidase. The two enzymatic activities detected in HIC1_NR were not caused by the saturation of the column, fact that was confirmed by reloading the column with this sample (data not shown). Regarding

Table 2
Summary of the purification balance of purified β-xylosidases/endo-xylanase/arabinofuranosidases from Fusarium pernambucanum MUM 18.62 extracellular media (EC0) following the flowpath schematised in Fig. 1.

Purification step	Sample name	Total protein (mg)	Total units (U)[a]			Yield (%)			Specific activity (U mg^{-1})[b]			Purification factor		
			β-xyl	E-xyl	Afur	β-xyl	E-xyl	Afur	β-xyl	E-xyl	Afur	β-xyl	E-xyl	Afur
Crude extract	EC0	992.4	33.67	2820.10	18.04	100.00	100.00	100.00	0.034	2.800	0.018	1.0	1.0	1.0
ASP	APS1_EC1	231.6	30.00	1193.80	14.52	89.11	42.33	80.52	0.159	6.300	0.077	4.7	2.2	4.2
HIC1	**HIC1_NR**	5.4 *	12.60	10.80	6.57	37.43	0.38	36.41	2.353	2.017	1.226	69.4	0.7	67.5
HIC2	HIC2_E1	2.9	5.85	0.54	1.58	17.39	0.02	8.75	1.628	0.150	0.439	48.0	0.1	24.2
	HIC2_E2	4.6	2.09	5.47	4.14	6.22	0.19	22.97	0.364	0.951	0.721	10.7	0.3	39.6
SEC1_A	SEC1_A_E1	1.8	1.61	0.09	0.31	6.00	0.00	2.17	0.883	0.048	0.171	26.0	0.0	9.4
SEC1_B	SEC1_B_E1	2.6	0.32	0.02	0.23	1.24	0.00	1.61	0.110	0.008	0.077	3.2	0.0	4.2
SEC2	SEC2_E1	0.3[c]	0.07	0.00	0.02	0.28	0.00	0.21	0.260[c]	0.000[c]	0.096[c]	7.7	0.0	5.3
	SEC2_E2	0.2[c]	0.02	0.00	0.02	0.10	0.00	0.13	0.120[c]	0.000[c]	0.083[c]	3.5	0.0	4.6
HIC1	**HIC1_E1**	4.4	0.38	0.64	0.41	1.4	0.03	2.9	0.084	0.150	0.092	2.5	0.1	5.1
SEC1_C	SEC1_C_E1	0.8	0.13	0.04	0.03	0.7	0.00	0.3	0.157	0.004	0.037	4.6	0.0	2.0
AEC	AEC_E1	-	-	-	-	-	-	-	-	-	-	-	-	-
	AEC_E2	-	-	-	-	-	-	-	-	-	-	-	-	-
HIC1	**HIC1_E2**	4.3	0.33	178.80	0.32	1.20	7.90	2.00	0.096	52.100	0.077	2.8	18.3	5.1
SEC1_D	SEC1_D_E1[d]	1.4[c]	0.22	127.33	0.13	0.80	5.60	1.00	0.163[c]	93.200[c]	0.097[c]	4.8	32.8	5.3
HIC1	**HIC1_E3**	4.8	0.18	253.04	0.19	0.70	11.60	8.80	0.050	74.190	0.050	1.6	26.1	24.2
SEC1_E	SEC1_E_E1[e]	1.1[c]	0.03	212.82	0.00	0.10	9.70	0.00	0.030[c]	199.960[c]	0.000[c]	0.8	70.4	0.0

Concentration steps were not included in purification balances as enzymatic activity recovery was over 95 %, irrespective of the concentration method employed.
β-xyl: β-xylosidase; *E*-xyl: Endo-xylanase; Afur: Arabinofuranosidase.
*An exhaustive dialysis step was needed to quantify protein in this extract, which may result in elimination of proteins with MM < 10 kDa (cut off of the membrane).
[a]Enzymatic activities were determined at 30 °C with 25 mM phosphate buffer, pH 8. Substrates: 2.5 mM pNP-X (for β-xyl); 1 % arabinoxylan (for E-xyl); 2.5 mM pNP-A (for Afur).
[b]Protein concentration was determined by BCA.
[c]Protein concentration was determined by measuring the absorbance at 280 nm with Thermo Scientific NanoDrop 2000c.
[d]*FpXylEAB*.
[e]*FpXynE*.

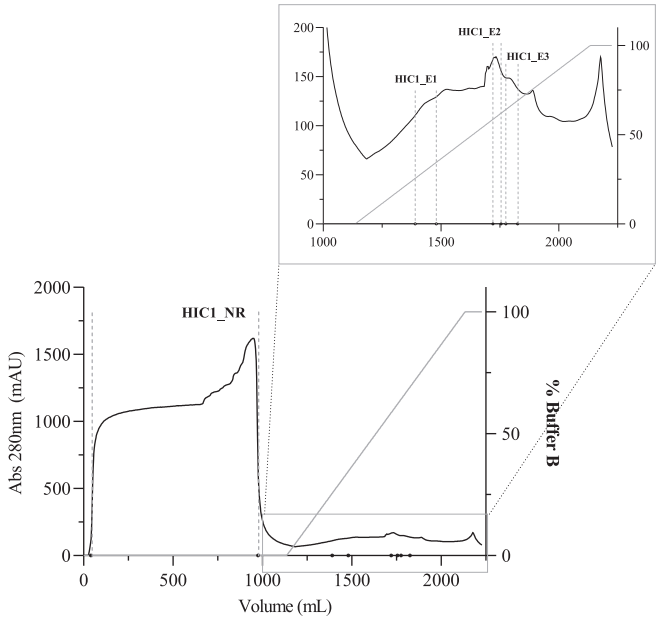

Fig. 3. Hydrophobic interaction chromatography (HIC1) using Phenyl Sepharose 6 FF column (50 mL) equilibrated with 50 mM phosphate buffer pH 6.8 and 1.7 M $(NH_4)_2SO_4$. Sample: 1.3 L (231.6 mg protein) of diluted supernatant resulted after 1.7 M $(NH_4)_2SO_4$ precipitation of *F. pernambucanum* MUM 18.62 extracellular proteins (ASP_EC0). Loading flow rate: 1.2 mL min^{-1}. Elution flow rate: 1.5 mL min^{-1}. Fractions: 5 mL. Grey line: % buffer B (50 mM phosphate buffer pH 6.8). Active fractions are indicated between dotted lines. Insert: Zoom of the chromatographic profile between 1000 and 2500 mL elution volume.

HIC1_E2 and HIC1_E3, both were active for the three evaluated activities: *endo*-xylanase, β-xylosidase and arabinofuranosidase.

All these fractions followed different purification steps that will be analysed in more detail in the following sections.

3.3.1.1. HIC1_E1 fraction. This fraction was positive for β-xylosidase and arabinofuranosidase activities, but with low recovery yields in relation to ASP_EC1 (around 1.4 and 2.9 %, respectively) (Table 2). Purification factor was 2.5 for β-xylosidase and 5.1 for arabinofuranosidase. HIC1_E1 (Fig. S3A, lane 4 – HIC1_E1) was further purified, first by size exclusion chromatography using a HiLoad® 16/60 Superdex® 75 prep grade column (SEC1_C, Fig. S1), and the active pooled fraction (Fig. S3A, lane 5 – SEC1_C_E1) was then purified by anion exchange chromatography on a MonoQ® 5/50 GL column (AEC, Fig. S2) to obtain samples AEC_E1 and AEC_E2 (Fig. 1).

AEC_E1 and AEC_E2 were again active for β-xylosidase and arabinofuranosidase, although enzyme and protein balances were not measured due to their low protein content and little volume resulting from the MonoQ® 5/50 GL column (Table 2, data not shown). By tricine SDS-PAGE (Fig. S3B), 5 and 3 protein bands were visualised for AEC_E1 and AEC_E2, respectively, with molecular masses (MMs) ranging from 195 to 86 kDa. These values are consistent with most of the described β-xylosidases, which exhibit molecular masses around 100 kDa [46].

Due to the difficulties of working with this sample regarding the low protein and enzymatic yields, we next focus on the non-retained fraction to the hydrophobic chromatography (HIC_NR), where β-xylosidase and arabinofuranosidase activities were also detected.

3.3.1.2. HIC1_NR fraction. As already indicated, HIC1_NR was active for β-xylosidase, arabinofuranosidase and *endo*-xylanase, although the purification factor for the latter decreased from 2.2 in ASP1_EC1 to 0.7 in HIC1_NR. Meanwhile, 37.43 % of the β-xylosidase and 36.41 % of the arabinofuranosidase activity from EC0 remained in HIC1_NR. Those activities were enriched by 69.4-fold and 67.5-fold, respectively (Table 2). Efforts to purify this fraction using anionic or cationic exchange chromatography were unsuccessful prompting us to revert to HIC. Additionally, HIC avoided time-consuming dialysis steps required to remove the $(NH4)_2SO_4$, which would have been necessary had ionic exchange chromatography been employed.

HIC1_NR fraction was concentrated (Fig. S7A, lane 4 – HIC1_NR), mixed with $(NH_4)_2SO_4$ to adjust its final concentration to that used in the equilibration buffer (2.2 M) of the following chromatography (HIC2, Fig. 1), centrifuged, and re-loaded onto the Phenyl Sepharose™ 6 FF column. Elution was performed following the methodology described in Section 2.4.2 (HIC2).

No activity was detected in the non-retained fraction (data not shown). Contrary, active fractions were detected at 25 % and 55 % elution buffer steps (Fig. S4) that were pooled and named HIC2_E1 and HIC2_E2, respectively (Fig. 1). Although both were active for β-xylosidase and arabinofuranosidase, the β-xylosidase activity previously detected in HIC1_NR was mainly recovered in fraction HIC2_E1 (17.39 %), whereas the arabinofuranosidase activity from HIC1_NR was mostly recovered in HIC2_E2 (22.97 %) (Table 2). Therefore, HIC2_E1 achieved a purification factor of 48 for β-xylosidase and 24.2 for arabinofuranosidase. Whereas HIC2_E2 achieved a purification factor of 10.7 and 39.9 for β-xylosidase and arabinofuranosidase, respectively (Table 2). Both samples were still active for *endo*-xylanase activity, but purification factors have been reduced throughout the purification steps.

Samples HIC2_E1 and HIC2_E2 were concentrated to 1.6 mL (2.9 mg protein in HIC2_E1 and 4.6 mg protein in HIC2_E2) by Amicon® Ultra centrifugal tubes with 10 kDa MWCO. Concentrated samples (Fig. S7A, lane 5 – HIC2_E1 and lane 7 – HIC2_E2) were again purified separately through size exclusion chromatography using HiLoad® 16/60 Superdex® 75 prep grade column (SEC1_A and SEC1_B, Fig. 1) as described in Section 2.4.3.

Profiles obtained from each chromatography are shown in Fig. S5, where active fractions (β-xylosidase and arabinofuranosidase) are indicated between dotted lines, close to the void volume of the column. The pooled active fractions were named SEC1_A_E1 (Fig. S5A) and SEC1_B_E1(Fig. S5B) which eluted well apart from several other contaminant proteins (probably associated to endo-xylanase enzyme and other not targeted proteins) with apparent lower MMs. Specific activities were higher for sample SEC1_A_E1 (β-xylosidase and arabinofuranosidase). Analysis by denaturing electrophoresis revealed two pools of bands in sample SEC1_A_E1 (Fig. S7A, lane 6); three with MM higher than 50 kDa also present in sample SEC1_A_E2 (Fig. S7A, lane 8). Bands with 40.0 and 48.4 kDa in the first sample were nearly undetected in the later. We selected SEC1_B_E1 to proceed with the purification which increased purification factor to 3.2 for β-xylosidase and 4.2 for arabinofuranosidase with recovery yields of 1.24 % and 1.61 %, respectively (Table 2).

Next purification step was again using SEC chromatography but with a HiPrep™ 16/60 Sephacryl® S-200 column that allows separating proteins from 5 kDa to 250 kDa (the range for the previous SEC column was 3 to 70 kDa). As before, SEC1_B_E1 was concentrated, and 4 mL (2.6 mg protein) was loaded onto the column (as indicated in Section 2.4.3 for SEC2 purification step (Fig. 1)).

The chromatographic profile (Fig. S6) shows protein absorbance at 280 nm together with β-xylosidase and arabinofuranosidase activities determined in the collected fractions (coloured lines). Both activities split into two peaks whose maxima did not parallel the protein peak. The first active fractions spread over a considerable region which might indicate the association of the enzymes with other molecules from the sample. Therefore, we focused on the second peaks resulting in samples SEC2_E1 (between 48.6 and 51.6 mL elution volume), and SEC2_E2 (between 53 and 55.6 mL elution volume) (Fig. S6). β-Xylosidase/arabinofuranosidase ratio was: 2.7 for SEC2_E1 and 1.4 for SEC2_E2 (Table 2), indicating that they were different enzymes as deduced form their SEC profile in Fig. S6. Accordingly, the purification factors and

specific activities, for both β-xylosidase and arabinofuranosidase, were improved compared to the previous chromatographic step (Table 2). Using tricine SDS-PAGE gels, SEC2_E1 showed at least 8 protein bands ranging from 47 to 188 kDa, whereas 1 major band (band J, 90 kDa) and two minor was (I and K bands) were visualised for SEC2_E2 (Fig. S7B).

According to their MM, two protein bands were common to the two samples; one with 104.0 ± 5.4 kDa (Fig. S7B, band D and I) and the second with 88.2 ± 4.2 kDa (Fig. S7B, band E and J), that might correspond to the detected β-xylosidase and arabinofuranosidase activities.

Although we were unable to purify to homogeneity these two enzymes, after two steps of hydrophobic interaction chromatography (HIC1 and HIC2) followed by two SEC chromatographic steps with different separation ranges (SEC1 and SEC2) (Fig. 1), we obtained two fractions, each of them enriched with β-xylosidase or arabinofuranosidase activity (SEC2_E1 and SEC2_E2) (Fig. 1).

Fusarium pernambucanum produced different β-xylosidases and arabinofuranosidases to hydrolise the beechwood xylan and corn cob xylan. This fact has been confirmed with *F. graminearum*, which expresses several xylanolytic enzymes to colonise plants [26].

The enzymes included in the different isolated pools (AEC1, AEC2, SEC2_E1 and SEC2_E2) possess comparable molecular masses but different hydrophobicity. In addition to the detected enzymes in these samples, many other minor β-xylosidases and arabinofuranosidases might be present, as we were able to recover just over 6 % of the activities quantified in EC0 (Table 2). Actually, most of the purification protocols used in literature to isolate extracellular β-xylosidases and arabinofuranosidases by chromatographic procedures do not usually reach recovery yields higher than 13 % [47–51].

Protein bands detected in AEC1, AEC2, SEC2_E1 and SEC2_E2 (Fig. S3B and Fig. S7B) were cut and submitted to in-gel digestion and peptide-mass fingerprinting identification, results that are described in Section 2.8.

3.3.1.3. HIC1_E2 fraction. HIC1_E2 pool obtained from HIC1 (Figs. 1 and 3) was active for the three measured activities, β-xylosidase, arabinofuranosidase, and *endo*-xylanase (Table 2). Their specific activity increased as it did the purification factor (in relation to EC0): 32.8-fold for endo-xylanase activity, 4.2-fold for arabinofuranosidase, and 4.7-fold for β-xylosidase activity. (Table 2).

To separate the enzymes responsible for the three activities in HIC1_E2 (Fig. 6, lane 4 – HIC1_E2), the collected pool was concentrated to 1.5 mL (3.2 mg protein) as usual, loaded onto HiPrep^{R} 16/60 Superdex^{R} 75 column (SEC1_D, Fig. 1), and eluted as indicated in Section 2.4.3.

The chromatographic profile, as well as active fractions (coloured lines) are included in Fig. 4. A main protein peak was obtained after SEC1_D that paralleled the three enzymatic activities examined (β-xylosidase, arabinofuranosidase, and *endo*-xylanase), which reached their respective maxima at the same volume.

Those active fractions eluted between 66.3 and 75.3 mL were pooled and analysed by SDS-PAGE in 10 % acrylamide gels where only one band at 39.9 kDa was detected (Fig. 6B, lane 6 – SEC1_D_E1). To confirm if the 39.9 kDa protein was responsible for two of the three activities, we attempted zymographic analysis for *endo*-xylanase and β-xylosidase activity. However, we failed to re-naturalise the enzyme in the SDS-PAGE gels and no activity was detected on native PAGE gels (data not shown).

Protein bands detected in SEC1_D_E1 (Fig. 6C, bands A-B-C) were submitted to peptide-mass fingerprinting identification, results that are included in Section 3.4.

3.3.1.4. HIC1_E3 fraction. HIC1_E3 fraction (Fig. 1) obtained from HIC1 (Figs. 1 and 3) was active for the three measured activities, β-xylosidase, arabinofuranosidase, and *endo*-xylanase. Their specific activity increased in the HIC1_E3 pool (Table 2) as did the purification factor (in relation to EC0): 26.1-fold for *endo*-xylanase, 1.6-fold for β-xylosidase and 24.2-fold for arabinofuranosidase.

To purify the enzymes responsible for these activities, the HIC1_E3 fraction (Fig. 6A, lane 5 – HIC1_E3) was concentrated as usual to 1.5 mL (3.3 mg protein) and loaded onto HiLoad® 16/60 Superdex® 75 column (SEC1_E, Fig. 1) eluted as indicated in Section 2.4.3.

The chromatographic profile displayed a symmetric peak between 82 and 93 mL volume elution which was analysed for β-xylosidase, arabinofuranosidase, and endo-xylanase activities (Fig. 5). Yet, fractions were only active for endo-xylanase activity, matching the highest endo-xylanase activity and protein content at the same volume, which suggested that the enzyme could be pure. Active samples were pooled, concentrated, and tested again against the pNP-X and pNP-A substrates, finding some residual β-xylosidase activity (17 % of the loaded activity units in SEC1_E step) but no arabinofunarosidase activity (Table 2).

Contrary, 84 % of the *endo*-xylanase activity units were recovered after the chromatographic step. These results strongly suggested that the SEC1_E_E1 sample was mainly an endo-xylanase with minor amounts of contaminant β-xylosidase. This conclusion was supported by the

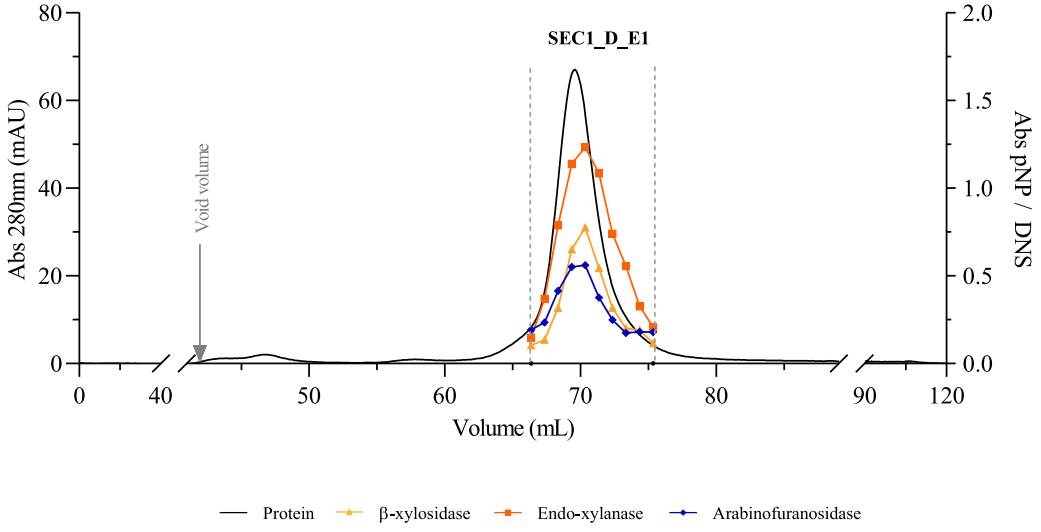

Fig. 4. Size exclusion chromatography (SEC1_D) using HiLoad® 16/60 Superdex® 75 prep grade column. Sample: 1.5 mL (4.3 mg protein) of concentrated HIC1_E2 obtained from HIC1 chromatographic step. Loading flow rate: 0.3 mL min^{-1}. Elution flow rate: 0.3 mL min^{-1}. Elution buffer: 20 mM phosphate buffer pH 7.0, 150 mM NaCl and 0.05 % sodium azide Fractions: 0.5 mL. Active fractions are indicated between dotted lines.

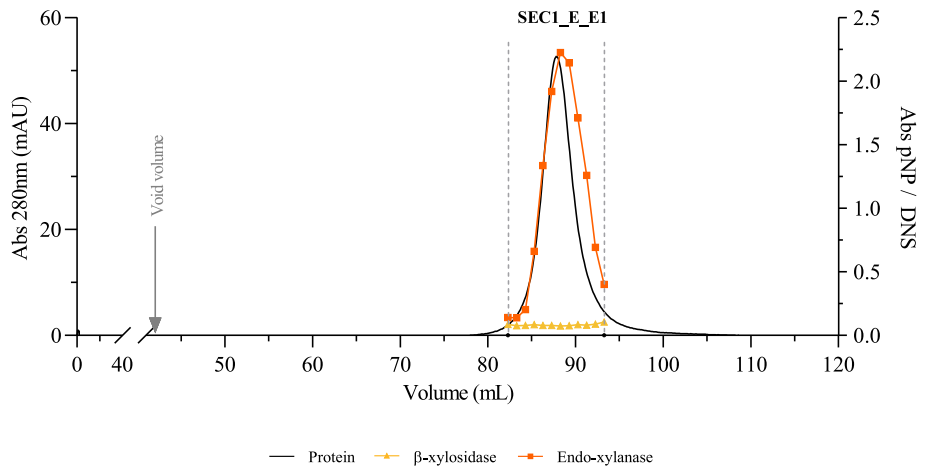

Fig. 5. Size exclusion chromatography (SEC1_E) using HiLoad® 16/60 Superdex® 75 prep grade column. Sample: 1.5 mL (4.8 mg protein) of concentrated HIC1_E3 obtained from HIC1 chromatographic step. Loading flow rate: 0.3 mL min^{-1}. Elution flow rate: 0.3 mL min^{-1}. Elution buffer: 20 mM phosphate buffer pH 7.0, 150 mM NaCl and 0.05 % sodium azide Fractions of 0.5 mL. Active fractions are indicated between dotted lines.

detection in this sample of a single protein band by electrophoresis on SDS-PAGE (Fig. 6B) and Tricine gels (Fig. 6C, lane 3 – SEC1_E_E1), whose MM was estimated as 18 kDa, and confirmed as *endo*-xylanase by renaturing zymography on SDS-PAGE gels supplemented with 0.5 % (*w/v*) arabinoxylan (Fig. 6B, lane 8). That MM may indicate that belongs to GH11 family as the MM of endo-xylanases from this family is usually lower than 20 kDa [63]. This was further confirm by peptide-mass fingerprinting analysis (Section 3.4).

3.4. Identification: peptide-mass fingerprinting

Final samples resulted from each purification flow path were identified by peptide-mass fingerprinting. In this case, samples were analysed by denaturing gradient electrophoresis using Novex 10 to 20 % Tricine gels which usually give better band resolution. Bands were visualised with Colloidal Coomassie Blue G-250, manually excised and digested with trypsin. The following bands were analysed: 8 from SEC2_E1 (Fig. S7B, lane 9), 3 from SEC2_E2 (Fig. S7B, lane 10), 5 from AEC_E1 (Fig. S3B, lane 6), 3 from AEC_E2 (Fig. S3B, lane 7), 3 from SEC1_D_E1 (Fig. 6C, lane 7), and 1 from SEC1_E_E1 (Fig. 6C, lane 7).

Peptide-mass fingerprinting was carried out and data searched against Swiss-Prot. Currently, fungi (taxon ID 4751) have 36,254 reviewed sequences, where just 112 belong to endo-xylanase, 22 to β-xylosidase and 38 to arabinofuranosidase. Among them only 6 endo-xylanases belong to *Fusarium* genera and any reviewed β-xylosidase or arabinofuranosidases. Therefore, search was also performed against unreviewed sequences (TrEMBL) for *Fusarium* genera (taxon ID 5506).

3.4.1. Bands identified from SEC2_E1 and SEC2_E2 purified samples

When the search was made against reviewed sequences, 4 of the 11

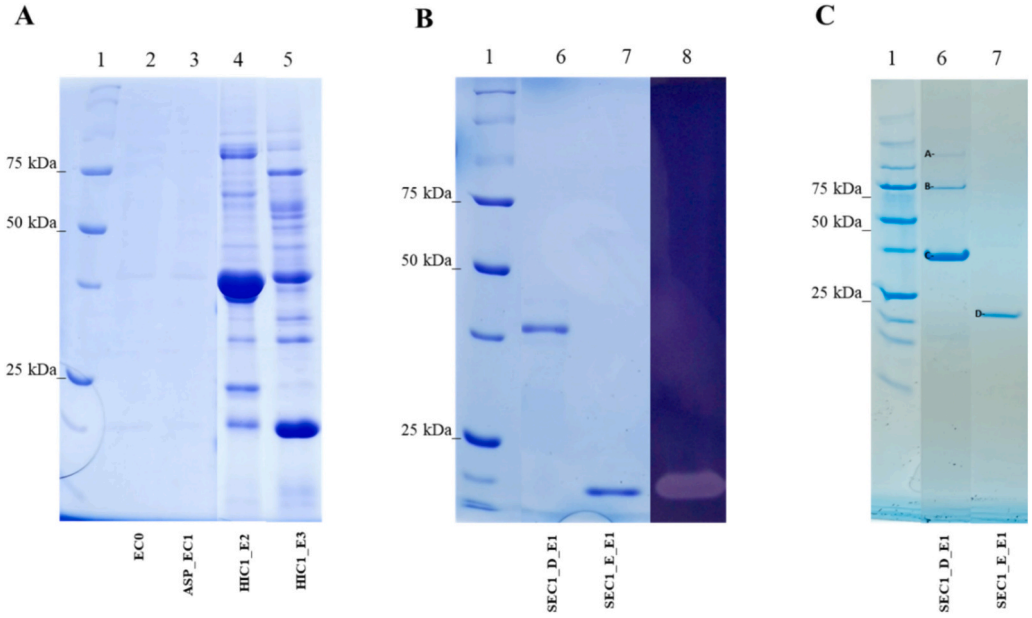

Fig. 6. Denaturing gels of *Fusarium pernambucanum* enzymatic extracts corresponding to HIC1_E2 and HIC1_E3 samples and those thereafter (Fig. 1). (A) SDS-PAGE using 12 % polyacrylamide gels stained with Coomassie Brilliant Blue R-250; (B) SDS-PAGE using 10 % polyacrilamide gels including 0.5 % (w/v) arabinoxylan for endo-xylanase activity detection. (C) Novex 10 to 20 % Tricine gels stained with Colloidal Coomassie G-250. Capital letters (from A to D) points bands submitted to peptide-mass fingerprinting analysis. Lane 1: Precision plus protein unstained standards; Lane 2: EC0; Lane 3: ASP_EC1; Lane 4: HIC1_E2; Lane 5: HIC1_E3; Lane 6: SEC1_D_E1 (FpXylEAB); Lane 7: SEC1_E_E1 (FpXynE); Lane 8: Zymogram of SEC1_E_E1 (FpXynE). After electrophoresis, gel was renatured in 25 mM citrate-phosphate buffer (pH 6.0) with 2.5 % (v/v) Triton X-100 for 30 min at RT.

bands isolated from SEC2_E1 (Fig. S7B, lane 9) and SEC2_E2 (Fig. S7B, lane 10) matched an endo-xylanase enzyme (accession number: I1RQU5). However, only 2 to 4 peptides matched the template sequence (I1RQU5) and none of the peptides matched β-xylosidases or arabinofuranosidases.

When search was made against unreviewed sequences, different enzymes matched proteins from SEC2_E1 and SEC2_E2 samples: β-glucosidase, α-glucosidase, β-xylanase, carboxyl esterase, β-xylosidase and α-arabinofuranosidase.

As it was previously stated, SEC2_E1 and SEC2_E2 samples were positive for β-xylosidase/α-arabinofuranosidase (Table 2). As for β-glucosidase activity, both samples showed no activity (data not shown), and α-glucosidase and carboxyl esterase activity were not tested. Following this, band E showed 33 % coverage (14 peptides) for bi-functional β-xylosidase/α-arabinofuranosidase predicted sequence from *F. coffeatum* (A0A366S3H5), 15.2 % coverage (8 peptides) for α-arabinofuranosidase predicted sequence from *F. poae* (A0A1B8AB40) and 14.8 % coverage (8 peptides) for α-arabinofuranosidase predicted sequence from *F. flagelliforme* (A0A395M5W6). Similar results were achieved for band J with 28.9 % coverage (9 peptides) for bi-functional β -xylosidase/α-arabinofuranosidase predicted sequence from *F. coffeatum* (A0A366S3H5) and 14.8 % coverage (7 peptides) α-arabinofuranosidase predicted sequence from *F. coffeatum* (A0A366S3H5). Except for the bi-functional β-xylosidase/α-arabinofuranosidase predicted sequence from *F. coffeatum* (A0A366S3H5), none of the peptides from the different bands in SEC2_E1 and SEC2_E2 samples matched β –xylosidase sequences.

3.4.2. Bands identified from AEC_E1 and AEC_E2 purified samples

Peptides generated from proteins isolated from samples AEC_E1 and AEC_E2 (Fig. S3B) matched sequences from β-glucanases, from both, reviewed and unreviewed sequences. However, we again analysed samples AEC_E1 and AEC_E2 for β-glucanases activity with negative results (data not shown).

The number of reviewed sequences for β-glucanases largely exceeds those of β-xylosidase and α/β-arabinofuranosidase (619 vs 85–88). Attending to unreviewed sequences from *Fusarium* genera, 4135 sequences have been confirmed as β-glucanase but for β-xylosidase and α/β-arabinofuranosidase only 1421 and 1023 respectively. Thus, the failure to fully identify the targeted enzymes in samples SEC2_E1, SEC2_E2, AEC_E1 and AEC_E1 may likely be caused by the low number of β-xylosidases and arabinofuranosidases described in the literature, and hence of sequences included in databases.

3.4.3. Bands identified from SEC1_D_E1 purified sample

A main protein band was estimated at 39.9 kDa (Fig. 6C, lane 6, band C). Bands A and B resulted in MM of 79.3 and 119.4 kDa, respectively, which fitted with expected MM for dimers and trimers of the 39.9 kDa protein. Although denaturing conditions were used for Tricine gel (SDS and β-ME were added to the sample buffer), the incubation at 85 °C for 2 min (following manufacturer's specification) may result in an incomplete separation of the monomeric forms, resulting in less intense bands with double and triple MM. When SDS-PAGE in 10 % acrylamide gel was performed (Fig. 6B, lane 6), only the band at 39.9 kDa was detected.

The generated peptides from sample SEC1_D_E1 (bands A, B and C), isolated from HIC1_E2, matched sequences of GH10 xylanases (Fig. S8). The MS data of band C (Fig. 6B, lane 6) provided 41.2 % coverage (17 peptides) for Xyl1 (I1RQU5) and 33.0 % coverage (9 peptides) for Xylanase A or Xylanase III (B3A0S5). However, higher coverages were achieved for predicted xylanase sequence from *Fusarium coffeatum* (A0A366S360): 59. % coverage (29 peptides). All of them show MM ranging from 36 to 40 kDa.

With increasing MM (Fig. 6B, bands A and B), sequence coverage decreased, i.e. band A had 27.2 % coverage (10 peptides) and band B had 45.2 % coverage (14 peptides), both against the predicted xylanase from *Fusarium coffeatum* (A0A366S360). Nevertheless, they once again matched the three same templates as the monomeric protein (band C).

The SEC1_D_E1 enzyme, that was renamed as *FpXylEAB*, was a trifunctional xylanolytic enzyme that hydrolyzed several substrates associated to different activities: pNP-X and MUX (β-xylosidase activity), pNP-A (arabinofuranosidase activity) and arabinoxylan (*endo*-xylanase activitiy). SEC1_D_E1 pool resulted specific activities of (U mg^{-1}) (quantified at 30 °C and pH 8): 0.163 β-xylosidase, 93.200 endo-xylanase and 0.097 arabinofuranosidase. The β-xylosidase/arabinofuranosidase activity relation was 1.7.

Bifunctional enzymes with different xylanolytic activities have been broadly studied and even grouped into glycosyl hydrolase (GH) families with two catalytic domains (GH16, 61, and 62) or with secondary xylanolytic activities (GH9, 12, 26, 30 and 44) [52]. However, some *Fusarium* species have been described as producers of bifunctional xylanolytic enzymes belonging to other GH families: GH43 bifunctional β-xylosidase and α -L-arabinofuranosidase [53], GH27 bifunctional α-D-galactopyranosidase, β-L-arabinofuranosidase [54], GH11 bifunctional *endo*-xylanase and β-xylosidase (Table 4) [55], and GH10 bifunctional *endo*-xylanase and β-xylosidase (Table 4) [7]. Even a trifunctional enzyme active for endo-xylanase, cellulose, and transferase has been described for *Fusarium commune* (Table 4) [56]. However, to our knowledge, this is the first trifunctional enzyme active for *endo*-xylanase, β-xylosidase and arabinofuranosidase described within the *Fusarium* genera, and the fifth reported in the literature, after *PcAxy43B* enzyme from *Paenibacillus curdlanolyticus* [57–59], *Ttxy43* from *Thermothelomyces thermophile* [60], and two recombinant enzymes constructed by linking catalytic domains [61,62].

3.4.4. Bands identified from SEC1_E_E1 purified sample

Peptides generated from sample SEC1_E_E1 (Fig. 6C, band D) isolated from HIC1_E3 fraction, matched sequences of GH11 xylanases (Fig. S9). The MS data of band D (Fig. 6C, lane 7) provided 60 % coverage (51 peptides) for XylB (I1RII8). Again, higher coverage was achieved for predicted xylanase sequence from *Fusarium flagelliforme* (A0A395MKC9): 76 % coverage (49 peptides). Both enzymes showed MM of 24.5–24.6 kDa, slightly higher than that predicted for SEC1_E_E1 (Fig. 6B, 18 kDa).

Thereafter SEC1_E_E1 was renamed as *FpXynE*. The enzyme, with a specific activity of 199.96 U mg^{-1} (quantified 30 °C and pH 8), was characterised in terms of optimal pH and temperature conditions for activity, and stability as shown in the next sections.

3.5. Biochemical characterisation of purified FpXylEAB and FpXynE enzymes

Endo-xylanase *FpXylEAB* and *FpXynE* were characterised in terms of optimun operating pH and temperature conditions, as well as thermal and operational stability.

3.5.1. Effect of pH and temperature

The optimal pH and temperature conditions of *FpXylEAB* and *FpXynE* were quantified using arabinoxylan as substrate. The optimal pH was evaluated between 4 and 10 at 30 °C and temperature between 40 and 80 °C at the optimal pH.

FpXylEAB showed maximum activity at pH 6, and nearly 50 % of its activity was retained at pH 9 at 30 °C. *FpXynE* maximum activity was quantified at pH 6–7, and it was more sensitive to pH increase in contrast with *FpXylEAB*, with only 15 % of residual activity at pH 9 (Fig. 7A).

Regarding temperature, 50 °C and 60 °C were the optimal conditions for *FpXynE* and *FpXylEAB endo*-xylanase activities, respectively (Fig. 7B). Both enzymes showed extreme sensitivity to temperature rise, with just 25 % activity remaining at 70 °C.

Those optimal conditions matched with most of the endo-xylanases isolated from *Fusarium* (Table 4). pH optima for activity ranged from 5.0 to 8.0. About temperature, most of the endo-xylanases optimally work between 40 and 55 °C. However, two of them showed thermophile

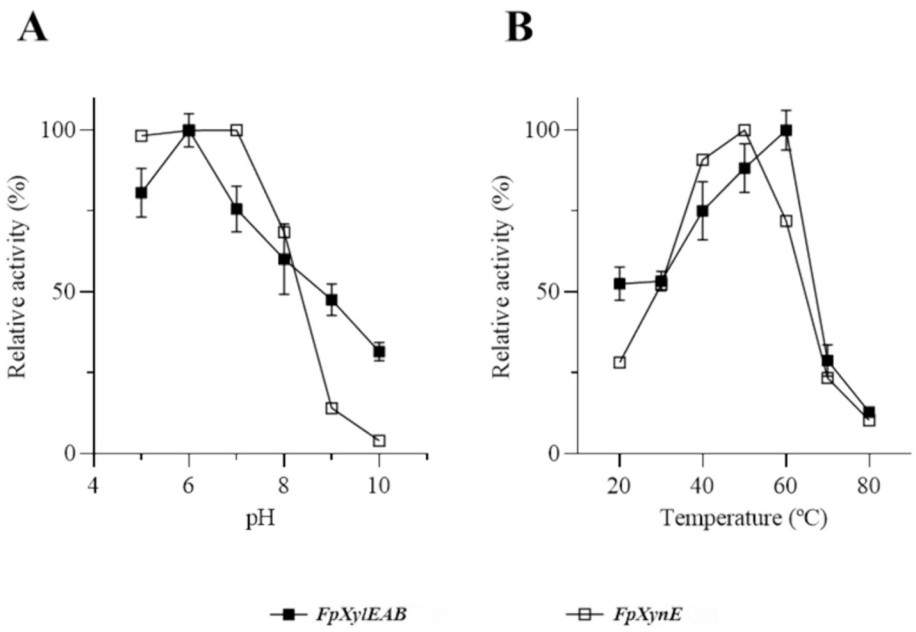

Fig. 7. (A) Optimal pH condition for *FpXylEAB* and *FpXynE* endo-xylanase activity. The effect of the pH was determined from 4.0 to 10.0 at 30 °C. Enzymatic activities are expressed as percentages of the max value: 100 % activity is 69.6 ± 1.9 U mg^{-1} for *FpXylEAB* and 160.3 ± 3.2 U mg^{-1} for *FpXynE*. (B) Optimal temperature condition for *pXylEAB* and *FpXynE* endo-xylanase activity. The effect of the temperature was determined from 20 °C to 80 °C at pH 6.0. Enzymatic activities are expressed as percentages of the max value: 100 % activity is 194.0 ± 2.4 U mg^{-1} for *FpXylEAB* and 343.3 ± 21.3 U mg^{-1} for *FpXynE*.

behavior with optimal activity at 60 °C: *FpXylEAB* from *F. pernambucanum* and Xylanase I from *F. oxysporum* (Table 4) Nonetheless, the optimal catalytic temperature of those later enzymes were 30 °C higher than the temperature used for their culture [18,64].

The endo-xylanase specific activity at optimal pH and temperature conditions for *FpXylEAB* (pH 6 and 60 °C respectively) and for *FpXynE* (pH 6 and 50 °C) were 194.0 ± 2.4 U mg^{-1} and 343.3 ± 21.3 U mg^{-1}, respectively, using arabinoxylan as substrate. β-Xylosidase and arabinofuranosidase activity of *FpXylEAB* at the optimal conditions were not measured because the self-hydrolysis of the pNP-X and pNP-A substrates at those conditions.

3.5.2. Thermal and operational stability

Thermal stability was assayed at pH 6.0 and 50 °C (*FpXynE*) or 60 °C (*FpXylEAB*). At these temperatures both enzymes were extremely unstable, with almost no detectable activity after 60 min incubation (Fig. 8, squares).

Nevertheless, it is known that xylans act as xylanase stabilisers against thermal inactivation either through substrate-catalytic site interactions or by carbohydrate binding modules [65,66]. In this sense, operational stability of each enzyme was evaluated by measuring the degree of hydrolysis of arabinoxylan in a buffered medium (Fig. 8, circles). The degree of hydrolysis was calculated as the product concentration measured at each time regarding the initial concentration of arabinoxylan in the reaction (10 mg mL^{-1}).

None of the enzymes were able to hydrolisemore than 8 % of the arabinoxylan after 60 min (Fig. 8).

According to the parametric values (Eqs. (1), (2), and (3)), *FpXynE* showed maximum degree of hydrolysis (H_m) 2-fold higher than that obtained with *FpXylEAB* after 60 min (Table 3). However, both *FpXylEAB* and *FpXynE* reached asymptotic phase before 30 min, at 23.3 min and 29.6 min, respectively (t_m, Table 3). This asymptotic behavior could be explained by enzyme inactivation, however, following thermal inactivation curves, at these times both enzymes still showed >50 % relative activity. These results may indicate that enzymes are still stable at the operational conditions (pH 6.0, and 50–60 °C), but product/substrate inhibition may occur at the t_m values.

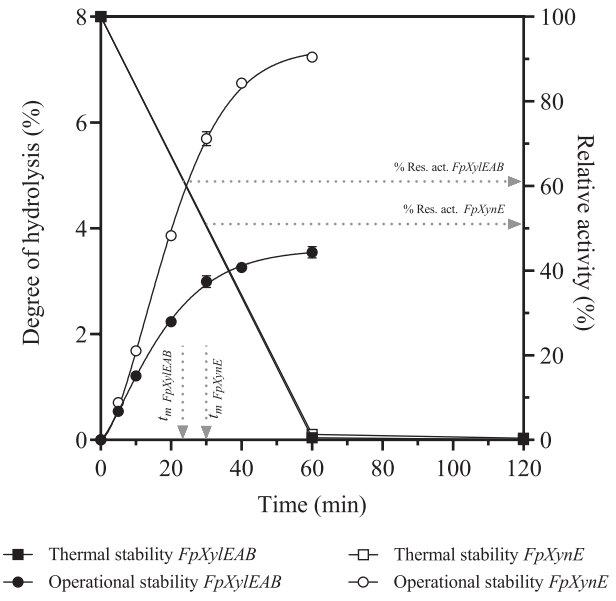

Fig. 8. Thermal stability (squares), expressed as percentages of the max endo-xylanase activity of FpXylEAB (black) and FpXynE (white). Operational stability (circles) measured as the product generation of FpXylEAB (black) and FpXynE (white) and expressed as percentage of the initial arabinoxylan concentration.

Table 3
Maximum degree of hydrolysis (H_m) and time required to achieve the beginning of asymptote phase (t_m), estimated from the Eqs. (1), (2) and (3).

	H_m (%)	t_m (min)	r^2-value
FpXynE	7.382 ± 0.029	29.638 ± 0.397	0.9991
FpXylEAB	3.595 ± 0.093	23.279 ± 0.536	0.9984

Table 4
Endo-xylanases identified from *Fusarium* species and their biochemical characteristics: optimal temperature and pH conditions for activity, and pH stability and its measurement conditions.

Fungi species	Name	Optimal activity conditions		pH stability*	Measurement conditions for pH stability	Reference
		T°	pH			
F. pernambucanum	*FpXylEAB*[a]	60 °C	6.0	–	–	This study
	FpXynE	50 °C	5.0–7.0	–	–	
F. graminarum	*Xyl1*	45–55 °C	6.0	5.5/8.5	5 h at 20 °C	[11]
	Xyl2	45–55°C[T]	6.0			
	XylA	40°C[T]	7.0-8.0	5.0–12.0	120 min at RT	[25]
	XylB	40°C[T]	7.0–8.0	2.0–12.0		
	XylC	40°C[T]	5.0–7.0	1.9–13.0		
	XylD	40°C[T]	5.0–7.0	5.0–12.0		
F. oxysporum	–[b]	50°C[T]	7.4	5.8-9.0	24 h at 40 °C	[56]
	Xylanase I	60 °C	6.0	9.0–10.0	24 h at 30 °C	[18]
	Xylanase II	55 °C	6.0	7.0–9.0		
	Xylanase III *FoXyn10*[a]	45°C[T]	6.0–8.0	7.0-10.0	24 h at 20 °C	[13,16]
	Xyl2[c]	40°C[T]	6.0	–	–	[55]
	Xyn11A	45 °C	6.0	5.0–11.0		
F. sp. 21	*Xyn11B*	45 °C	6.0	5.0–11.0	24 h at 4 °C	[67]
	Xyn11C	45 °C	5.0	2.0–11.0		
	Xyl10A	50 °C	6.0	6.0–11.0		
F. commune	*Xyl10B*[c]	50 °C	6.0	5.0–11.0	1 h at 4 °C	[7]
	Xyl11	50 °C	5.0	6.0–8.0		
F. proliferatum	–	55 °C	5.0–5.5	3.0–8.0	1 h at 40 °C	[17]
F. verticillioides	–	50 °C	5.5	4.5–10.0	30 min at 50 °C	[15]

– Data no available.
[T] Thermostable: >50 °C relative activity at the optimal condition after 1 h incubation.
[a] Trifunctional: *endo*-xylanase, β-xylosidase, arabinofuranosidase.
[b] Trifunctional: endo-xylanase, cellulase, transferase.
[c] Bifunctional: endo-xylanase, β-xylosidase.

Most of the xylanases included in Table 4 also resulted in low thermal stability at their optimal temperature, with <50 % relative activity after 60 min incubation. Even Xylanase I from *F. oxysporum*, whose optimal working condition was 60 °C, retained 47 % of its activity after 60 min incubation at 45 °C [18]. Operational stability was not determined for any of the xylanases summarised in Table 4.

Most xylanases included in Table 4 have been stated as alkali stable as they maintain >50 % activity at pH 9–10 when incubated for different periods of time. However, the incubations are made at very low temperatures (4–20 °C), far from those normally used when working with lignocellulosic materials [7,11,67]. Indeed, this could be a misleading information when the xylanases are studied in conditions at which they are not even active (or marginally active). For example, Dong et al. [11] based the stability of *F. graminearum* Xyl1 and Xyl2 on the fact that they lose 20 % of their activity after 5 h incubation at pH 5.5 and 8.5 at 20 °C. However, at 20 °C these enzymes shown <10 % of the activity at their optimum, which is around 45–55 °C. Similar results were claimed by Pollet et al. [25] for XylA, XylB, XylC and XylD from *F. graminearum*, which kept active after 120 min incubation at room temperature with pHs up to pH 13. Among all the xylanases included in Table 4, only XylA from *F. graminearum* showed >50 % relative activity at pH 9 at its optimal temperature condition [25]. Following this, stability on alkaline solutions was not analysed in the present study. Optimal pH condition was measured at 30 °C (Fig. 7A), temperature at which both enzymes still kept 50 % relative activity (Fig. 7B). However, as both enzymes showed <50 % activity at pH above 9 at 30 °C (Fig. 7), stability at alkaline conditions at the optimal temperatures for activity (50–60 °C) was not expected.

FpXylEAB and *FpXynE* were active at neutral pH but showed moderate thermophile characteristics. The improvement of their thermostability in presence of substrate makes them suitable to be included in the biorefinery for xylooligosaccharides production from lignocellulosic materials. Particularly, the trifunctional activity of *FpXylEAB* may be useful to increase the yield of prebiotic XOS (X_2-X_4), as it is able to act on both, long (arabinoxylan) and small substrates (pNP-X and pNP-A). However, deeper studies on substrate specificity and product release are now being performed to evaluate the suitability and the adequate hydrolysis conditions in order to maintain at minimum the monomer release.

4. Conclusions

The production of extracellular β-xylosidases by different crop pathogen fungi was determined. Among them, *Fusarium pernambucanum* MUM 18.62 strain showed the highest activity, and this activity was similar at acidic and alkaline conditions. β-xylosidase and endo-xylanase expression was influenced by the pre-inoculum media composition, resulting in higher expression when xylan was included as carbon source in the agar plates.

The resulted extracellular xylanotic enzymes were sequentially purified to isolate different pools with different activities: four pools active for β-xylosidase/arabinofuranoside, one pure trifunctional endo-xylanase/β-xylosidase/arabinofuranoside enzyme with molecular mass of 39.8 kDa (*FpXylEAB*) and one pure endo-xylanase with molecular mass of 18.0 kDa (*FpXynE*). Pure enzymes were highly active at pH 5–6 and 50–60 °C. Their stability was improved by the presence of arabinoxylan.

CRediT authorship contribution statement

Andrea Rodríguez-Sanz: Writing – review & editing, Writing – original draft, Methodology, Data curation. **Clara Fuciños:** Writing – review & editing, Project administration, Methodology. **Célia Soares:** Writing – review & editing, Methodology, Data curation. **Ana M. Torrado:** Project administration, Methodology, Conceptualization. **Nelson Lima:** Writing – review & editing, Methodology, Conceptualization. **María L. Rúa:** Writing – review & editing, Writing – original draft, Project administration, Methodology, Conceptualization.

Declaration of competing interest

The authors declare that they have no known competing financial interests or personal relationships that could have appeared to influence

the work reported in this paper.

Acknowledgement

This work was supported by the Spanish Ministry of Science and Innovation (RTI2018–099249-B-I00, PRODIXOS). Funding for open access charge: University of Vigo/CISUG. A. Rodriguez-Sanz thank to the Iacobus program (GNP-AECT) for the three-month research stay at the Centre of Biological Engineering of the Universidade do Minho (Portugal).

Appendix A. Supplementary data

Supplementary data to this article can be found online at https://doi.org/10.1016/j.ijbiomac.2024.132722.

References

[1] R.D. Singh, J. Banerjee, A. Arora, Prebiotic potential of oligosaccharides: a focus on xylan derived oligosaccharides, Bioact. Carbohydrates Diet. Fibre. 5 (2015) 19–30, https://doi.org/10.1016/j.bcdf.2014.11.003.

[2] A. Rodríguez-Sanz, C. Fuciños, A.M. Torrado, M.L. Rúa, Extraction of the wheat straw hemicellulose fraction assisted by commercial endo-xylanases. Role of the accessory enzyme activities, Ind. Crop. Prod. 179 (2022) 114655, https://doi.org/10.1016/j.indcrop.2022.114655.

[3] C. Amorim, S.C. Silvério, K.L.J. Prather, L.R. Rodrigues, From lignocellulosic residues to market: production and commercial potential of xylooligosaccharides, Biotechnol. Adv. 37 (2019) 107397, https://doi.org/10.1016/j.biotechadv.2019.05.003.

[4] A. Rohman, B.W. Dijkstra, N.N.T. Puspaningsih, β-Xylosidases: structural diversity, catalytic mechanism, and inhibition by monosaccharides, Int. J. Mol. Sci. 20 (2019) 7–11, https://doi.org/10.3390/ijms20225524.

[5] J.A. Linares-Pasten, A. Aronsson, E.N. Karlsson, Structural considerations on the use of endo-xylanases for the production of prebiotic xylooligosaccharides from biomass, Curr. Protein Pept. Sci. 19 (2016) 48–67, https://doi.org/10.2174/1389203717666160923155209.

[6] L. Lange, K. Barrett, A.S. Meyer, New method for identifying fungal kingdom enzyme hotspots from genome sequences, J. Fungi. 7 (2021) 207, https://doi.org/10.3390/jof7030207.

[7] Y. Huang, P.K. Busk, L. Lange, Cellulose and hemicellulose-degrading enzymes in *Fusarium commune* transcriptome and functional characterization of three identified xylanases, Enzyme Microb. Technol. 73–74 (2015) 9–19, https://doi.org/10.1016/j.enzmictec.2015.03.001.

[8] L.C. Bertonha, M. Leal Neto, J.A.A. Garcia, T.F. Vieira, R. Castoldi, A. Bracht, R. M. Peralta, Screening of *Fusarium* sp. for xylan and cellulose hydrolyzing enzymes and perspectives for the saccharification of delignified sugarcane bagasse, Biocatal. Agric. Biotechnol. 16 (2018) 385–389, https://doi.org/10.1016/j.bcab.2018.09.010.

[9] C. Peremore, B. Wingfield, Q. Santana, S. E.T., T.E. Motaung, Biofim characterization in the maize pathogen, *Fusarium verticillioides*, BioRxiv (2022), https://doi.org/10.1101/2022.11.18.517162.

[10] J. Jaroszuk-Ściseł, A. Nowak, I. Komaniecka, A. Choma, A. Jarosz-Wilkołazka, M. Osińska-Jaroszuk, R. Tyśkiewicz, A. Wiater, J. Rogalski, Differences in production, composition, and antioxidant activities of exopolymeric substances (EPS) obtained from cultures of endophytic *Fusarium culmorum* strains with different effects on cereals, Molecules 25 (2020) 1–33, https://doi.org/10.3390/molecules25030616.

[11] X. Dong, S.W. Meinhardt, P.B. Schwarz, Isolation and characterization of two endoxylanases from *Fusarium graminearum*, J. Agric. Food Chem. 60 (2012) 2538–2545, https://doi.org/10.1021/jf203407p.

[12] T. Cesar, V. Mrša, Purification and properties of the xylanase produced by *Thermomyces lanuginosus*, Enzyme Microb. Technol. 19 (1996) 289–296, https://doi.org/10.1016/0141-0229(95)00248-0.

[13] M. Dimarogona, E. Topakas, P. Christakopoulos, E.D. Chrysina, The structure of a GH10 xylanase from *Fusarium oxysporum* reveals the presence of an extended loop on top of the catalytic cleft, Acta Crystallogr. Sect. D Biol. Crystallogr. 68 (2012) 735–742, https://doi.org/10.1107/S0907444912007044.

[14] V.K. Gupta, R. Gaur, S.K. Yadava, N.S. Darmwal, Optimization of xylanase production from free and immobilized cells of *Fusarium solani* F7, BioResources 4 (2009) 932–945, https://doi.org/10.15376/biores.4.3.932-945.

[15] B.C. Saha, Xylanase from a newly isolated *Fusarium verticillioides* capable of utilizing corn fiber xylan, Appl. Microbiol. Biotechnol. 56 (2001) 762–766, https://doi.org/10.1007/s002530100716.

[16] P. Christakopoulos, W. Nerinckx, D. Kekos, B. Macris, M. Claeyssens, The alkaline xylanase III from *Fusarium oxysporum* F3 belongs to family F/10, Carbohydr. Res. 302 (1997) 191–195, https://doi.org/10.1016/S0008-6215(97)00075-X.

[17] B.C. Saha, Production, purification and properties of xylanase from a newly isolated *Fusarium proliferatum*, Process Biochem. 37 (2002) 1279–1284, https://doi.org/10.1016/S0032-9592(02)00012-2.

[18] P. Christakopoulos, W. Nerinckx, D. Kekos, B. Macris, M. Claeyssens, Purification and characterization of two low molecular mass alkaline xylanases from *Fusarium oxysporum* F3, J. Biotechnol. 51 (1996) 181–189, https://doi.org/10.1016/0168-1656(96)01619-7.

[19] L. Anand, S. Krishnamurthy, P.J. Vithayathil, Purification and properties of xylanase from the thermophilic fungus, *Humicola lanuginosa* (Griffon and Maublanc) Bunce, Arch. Biochem. Biophys. 276 (1990) 546–553, https://doi.org/10.1016/0003-9861(90)90757-P.

[20] M. Dubois, K.A. Gillis, J.K. Hamilton, P.A. Rebers, F. Smith, Colorimetric method for determination of sugars and related substances, Anal. Chem. 28 (1956) 350–356.

[21] M.J. Bailey, P. Biely, K. Poutanen, Interlaboratory testing of methods for assay of xylanase activity, J. Biotechnol. 23 (1992) 257–270, https://doi.org/10.1016/0168-1656(92)90074-J.

[22] J.A. Vázquez, J.M. Lorenzo, P. Fuciños, D. Franco, Evaluation of non-linear equations to model different animal growths with mono and bisigmoid profiles, J. Theor. Biol. 314 (2012) 95–105, https://doi.org/10.1016/j.jtbi.2012.08.027.

[23] J.A. Vázquez, M. Blanco, A.E. Massa, I.R. Amado, R.I. Pérez-Martín, Production of fish protein hydrolysates from scyliorhinus canicula discards with antihypertensive & antioxidant activities by enzymatic hydrolysis & mathematical optimization using response surface methodology, Mar. Drugs 15 (2017) 1–15, https://doi.org/10.3390/md15100306.

[24] T. Beliën, S. Van Campenhout, M. Van Acker, G. Volckaert, Cloning and characterization of two endoxylanases from the cereal phytopathogen *Fusarium graminearum* and their inhibition profile against endoxylanase inhibitors from wheat, Biochem. Biophys. Res. Commun. 327 (2005) 407–414, https://doi.org/10.1016/j.bbrc.2004.12.036.

[25] A. Pollet, T. Beliën, K. Fierens, J.A. Delcour, C.M. Courtin, Enzyme and Microbial Technology *Fusarium graminearum* Xylanases Show Different Functional Stabilities, Substrate Specificities and Inhibition Sensitivities 44, 2009, pp. 189–195, https://doi.org/10.1016/j.enzmictec.2008.12.005.

[26] D. Hatsch, V. Phalip, E. Petkovski, J.M. Jeltsch, *Fusarium graminearum* on plant cell wall: no fewer than 30 xylanase genes transcribed, Biochem. Biophys. Res. Commun. 345 (2006) 959–966, https://doi.org/10.1016/j.bbrc.2006.04.171.

[27] S. Saldarriaga-hernández, C. Velasco-ayala, P.L. Flores, M.D.J. Rostro-alanis, R. Parra-saldivar, M.N. Iqbal, D. Carrillo-nieves, Biotransformation of lignocellulosic biomass into industrially relevant products with the aid of fungi-derived lignocellulolytic enzymes, Int. J. Biol. Macromol. 161 (2020) 1099–1116, https://doi.org/10.1016/j.ijbiomac.2020.06.047.

[28] J.H.C. Woudenberg, J.Z. Groenewald, M. Binder, P.W. Crous, Alternaria redefined, Stud. Mycol. 75 (2013) 171–212, https://doi.org/10.3114/sim0015.

[29] D.N.X. Salmon, M.R. Spier, C.R. Soccol, L.P. de S. Vandenberghe, V. Weingartner Montibeller, M.C.J. Bier, V. Faraco, Analysis of inducers of xylanase and cellulase activities production by *Ganoderma applanatum* LPB MR-56, Fungal Biol. 118 (2014) 655–662, https://doi.org/10.1016/j.funbio.2014.04.003.

[30] S.R.M. Ibrahim, H. Choudhry, A.H. Asseri, M.A. Elfaky, S.G.A. Mohamed, G. A. Mohamed, Stachybotrys chartarum—a hidden treasure: secondary metabolites, bioactivities, and biotechnological relevance, J. Fungi. 8 (2022) 504, https://doi.org/10.3390/jof8050504.

[31] J. Cruz-Davila, J.V. Perez, D.S. del Castillo, N. Diez, *Fusarium graminearum* as a producer of xylanases with low cellulases when grown on wheat bran, Biotechnol. Reports. 35 (2022) e00738, https://doi.org/10.1016/j.btre.2022.e00738.

[32] R. Chouiter, I. Roy, C. Bucke, Optimisation of β-glucuronidase production from a newly isolated *Ganoderma applanatum*, J. Mol. Catal. B: Enzym. 50 (2008) 114–120, https://doi.org/10.1016/j.molcatb.2007.09.015.

[33] N.G. El Gamal, S.M.M. Atalla, R.R. El-Mohamedy, Improvement in potential of enzymes from Chaetomium globosum and Trichoderma harzianum using different agricultural wastes and applications, Biosci. Res. 15 (2018) 3977–3987.

[34] H.H. Azzaz, H.A. Murad, A.A. Aboamer, H. Alzahar, M. Fahmy, Cellulase production by fusarium graminearum and its application in ruminant's diets degradation, Pakistan, Aust. J. Biol. Sci. 23 (2020) 27–34, https://doi.org/10.3923/pjbs.2020.27.34.

[35] Q. An, X.J. Wu, M.L. Han, B.K. Cui, S.H. He, Y.C. Dai, J. Si, Sequential solid-state and submerged cultivation of the white rot fungus Pleurotus ostreatus on biomass and the activity of lignocellulolytic enzymes, BioResources 11 (2016) 8791–8805, https://doi.org/10.15376/biores.11.4.8791-8805.

[36] N. Kulkarni, A. Shendye, M. Rao, Molecular and biotechnological aspects of xylanases, FEMS Microbiol. Rev. 23 (1999) 411–456, https://doi.org/10.1016/S0168-6445(99)00006-6.

[37] R.P. De Vries, J. Visser, L.H. De Graaff, CreA modulates the XlnR-induced expression on xylose of Aspergillus niger genes involved in xylan degradation, Res. Microbiol. 150 (1999) 281–285, https://doi.org/10.1016/S0923-2508(99)80053-9.

[38] N. Najjarzadeh, L. Matsakas, U. Rova, P. Christakopoulos, Effect of oligosaccharide degree of polymerization on the induction of Xylan-degrading enzymes by *Fusarium oxysporum* f. sp. Lycopersici, Molecules 25 (2020), https://doi.org/10.3390/MOLECULES25245849.

[39] S. Malgas, M.S. Mafa, L. Mkabayi, B.I. Pletschke, A mini review of xylanolytic enzymes with regards to their synergistic interactions during hetero-xylan degradation, World J. Microbiol. Biotechnol. 35 (2019) 1–13, https://doi.org/10.1007/s11274-019-2765-z.

[40] O.M. Ontañon, S. Ghio, R. Marrero Díaz de Villegas, F.E. Piccinni, P.M. Talia, M. L. Cerutti, E. Campos, EcXyl43 β-xylosidase: molecular modeling, activity on natural and artificial substrates, and synergism with endoxylanases for lignocellulose deconstruction, Appl. Microbiol. Biotechnol. 102 (2018) 6959–6971, https://doi.org/10.1007/s00253-018-9138-7.

[41] F.M. Cunha, M.N. Esperança, C. Florencio, V.M. Vasconcellos, C.S. Farinas, A. C. Badino, Three-phasic fermentation systems for enzyme production with

sugarcane bagasse in stirred tank bioreactors: effects of operational variables and cultivation method, Biochem. Eng. J. 97 (2015) 32–39, https://doi.org/10.1016/j.bej.2015.02.004.
[42] F.M. Cunha, V.M. Vasconcellos, C. Florencio, A.C. Badino, C.S. Farinas, On-site production of enzymatic cocktails using a non-conventional fermentation method with agro-industrial residues as renewable feedstocks, Waste Biomass Valoriz. 8 (2017) 517–526, https://doi.org/10.1007/s12649-016-9609-y.
[43] C. Florencio, F.M. Cunha, A.C. Badino, C.S. Farinas, Validation of a novel sequential cultivation method for the production of enzymatic cocktails from trichoderma strains, Appl. Biochem. Biotechnol. 175 (2015) 1389–1402, https://doi.org/10.1007/s12010-014-1357-5.
[44] N. Bhardwaj, B. Kumar, K. Agarwal, V. Chaturvedi, P. Verma, Purification and characterization of a thermo-acid/alkali stable xylanases from *Aspergillus oryzae* LC1 and its application in Xylo-oligosaccharides production from lignocellulosic agricultural wastes, Int. J. Biol. Macromol. 122 (2019) 1191–1202, https://doi.org/10.1016/j.ijbiomac.2018.09.070.
[45] G. Fan, S. Yang, Q. Yan, Y. Guo, Y. Li, Z. Jiang, Characterization of a highly thermostable glycoside hydrolase family 10 xylanase from Malbranchea cinnamomea, Int. J. Biol. Macromol. 70 (2014) 482–489, https://doi.org/10.1016/j.ijbiomac.2014.07.025.
[46] Q.J. Yan, L. Wang, Z.Q. Jiang, S.Q. Yang, H.F. Zhu, L.T. Li, A xylose-tolerant β-xylosidase from *Paecilomyces thermophila*: characterization and its co-action with the endogenous xylanase, Bioresour. Technol. 99 (2008) 5402–5410, https://doi.org/10.1016/j.biortech.2007.11.033.
[47] B. Dong, H. Luo, B. Liu, W. Li, S. Ou, Y. Wu, X. Zhang, X. Pang, Z. Zhang, BcXyl, a β-xylosidase isolated from *Brunfelsia Calycina* flowers with anthocyanin-β-glycosidase activity, Int. J. Mol. Sci. 20 (2019), https://doi.org/10.3390/ijms20061423.
[48] H. Inoue, C. Kitao, S. Yano, S. Sawayama, Production of β-xylosidase from Trichoderma asperellum KIF125 and its application in efficient hydrolysis of pretreated rice straw with fungal cellulase, World J. Microbiol. Biotechnol. 32 (2016) 1–10, https://doi.org/10.1007/s11274-016-2145-x.
[49] F.I. Díaz-Malváez, B.E. García-Almendárez, A. Hernández-Arana, A. Amaro-Reyes, C. Regalado-González, Isolation and properties of β-xylosidase from *Aspergillus niger* GS1 using corn pericarp upon solid state fermentation, Process Biochem. 48 (2013) 1018–1024, https://doi.org/10.1016/j.procbio.2013.05.003.
[50] M. Wakiyama, K. Yoshihara, S. Hayashi, K. Ohta, Purification and properties of an extracellular β-xylosidase from Aspergillus japonicus and sequence analysis of the encoding gene, J. Biosci. Bioeng. 106 (2008) 398–404, https://doi.org/10.1263/jbb.106.398.
[51] M. Fritz, M.C. Ravanal, C. Braet, J. Eyzaguirre, A family 51 α-l-arabinofuranosidase from *Penicillium purpurogenum*: purification, properties and amino acid sequence, Mycol. Res. 112 (2008) 933–942, https://doi.org/10.1016/j.mycres.2008.01.022.
[52] N. Bhardwaj, B. Kumar, P. Verma, A detailed overview of xylanases: an emerging biomolecule for current and future prospective, Bioresour. Bioprocess. 6 (2019), https://doi.org/10.1186/s40643-019-0276-2.
[53] R. Carapito, C. Carapito, J.M. Jeltsch, V. Phalip, Efficient hydrolysis of hemicellulose by a *Fusarium graminearum* xylanase blend produced at high levels in *Escherichia coli*, Bioresour. Technol. 100 (2009) 845–850, https://doi.org/10.1016/j.biortech.2008.07.006.
[54] T. Sakamoto, Y. Tsujitani, K. Fukamachi, Y. Taniguchi, H. Ihara, Identification of two GH27 bifunctional proteins with β-L-arabinopyranosidase/α-D-galactopyranosidase activities from *Fusarium oxysporum*, Appl. Microbiol. Biotechnol. 86 (2010) 1115–1124, https://doi.org/10.1007/s00253-009-2344-6.
[55] S. Gómez, A.M. Payne, M. Savko, G.C. Fox, W.E. Shepard, F.J. Fernandez, M. Cristina Vega, Structural and functional characterization of a highly stable endo-β-1,4-xylanase from *Fusarium oxysporum* and its development as an efficient immobilized biocatalyst, Biotechnol. Biofuels 9 (2016) 1–19, https://doi.org/10.1186/s13068-016-0605-z.
[56] P. Christakopoulos, D. Kekos, B.J. Macris, M. Claeyssens, M.K. Bhat, Purification and characterisation of a major xylanase with cellulase and transferase activities from *Fusarium oxysporum*, Carbohydr. Res. 289 (1996) 91–104, https://doi.org/10.1016/0008-6215(96)00146-2.
[57] P. Limsakul, P. Phitsuwan, R. Waeonukul, P. Pason, C. Tachaapaikoon, K. Poomputsa, A. Kosugi, K. Ratanakhanokchai, A novel multifunctional arabinofuranosidase/endoxylanase/b-xylosidase GH43 enzyme from *Paenibacillus curdlanolyticus* B-6 and its synergistic action to produce arabinose and xylose from cereal arabinoxylan, Appl. Environ. Microbiol. 87 (2021), https://doi.org/10.1128/AEM.01730-21 e01730-21.
[58] T. Teeravivattanakit, S. Baramee, P. Phitsuwan, R. Waeonukul, P. Pason, C. Tachaapaikoon, Novel trifunctional xylanolytic enzyme Axy43A from *Paenibacillus*, Appl. Environ. Microbiol. 82 (2016) 6942–6951, https://doi.org/10.1128/AEM.02256-16.Editor.
[59] K. Wongratpanya, S. Imjongjairak, R. Waeonukul, S. Sornyotha, P. Phitsuwan, P. Pason, T. Nimchua, C. Tachaapaikoon, K. Ratanakhanokchai, Multifunctional properties of glycoside hydrolase family 43 from *Paenibacillus curdlanolyticus* strain B-6 including exo-β-xylosidase, endo-xylanase, and α-L-arabinofuranosidase activities, BioResources 10 (2015) 2492–2505, https://doi.org/10.15376/biores.10.2.2492-2505.
[60] A. Basit, T. Miao, J. Liu, J. Wen, L. Song, F. Zheng, H. Lou, W. Jiang, Highly efficient degradation of xylan into xylose by a single enzyme, ACS Sustain. Chem. Eng. 7 (2019) 11360–11368, https://doi.org/10.1021/acssuschemeng.9b00929.
[61] Y. Xue, J. Peng, R. Wang, X. Song, Construction of the trifunctional enzyme associating the *Thermoanaerobacter ethanolicus* xylosidase-arabinosidase with the *Thermomyces lanuginosus* xylanase for degradation of arabinoxylan, Enzyme Microb. Technol. 45 (2009) 22–27, https://doi.org/10.1016/j.enzmictec.2009.03.010.
[62] Z. Fan, K. Wagschal, W. Chen, M.D. Montross, C.C. Lee, L. Yuan, Multimeric hemicellulases facilitate biomass conversion, Appl. Environ. Microbiol. 75 (2009) 1754–1757, https://doi.org/10.1128/AEM.02181-08.
[63] J. Beaugrand, G. Chambat, V.W.K. Wong, F. Goubet, C. Rémond, G. Paës, S. Benamrouche, P. Debeire, M. O'Donohue, B. Chabbert, Impact and efficiency of GH10 and GH11 thermostable endoxylanases on wheat bran and alkali-extractable arabinoxylans, Carbohydr. Res. 339 (2004) 2529–2540, https://doi.org/10.1016/j.carres.2004.08.012.
[64] A.C. da S. Santos, J.V.C. Trindade, C.S. Lima, R. do N. Barbosa, A.F. da Costa, P. V. Tiago, N.T. de Oliveira, Morphology, phylogeny, and sexual stage of Fusarium caatingaense and *Fusarium pernambucanum*, new species of the Fusarium incarnatum-equiseti species complex associated with insects in Brazil, Mycologia 111 (2019) 244–259, https://doi.org/10.1080/00275514.2019.1573047.
[65] R.D. Barabote, J.V. Parales, Y.Y. Guo, J.M. Labavitch, R.E. Parales, A.M. Berry, Xyn10A, a thermostable endoxylanase from acidothermus cellulolyticus 11B, Appl. Environ. Microbiol. 76 (2010) 7363–7366, https://doi.org/10.1128/AEM.01326-10.
[66] C. Pandey, P. Sharma, N. Gupta, Engineering to enhance thermostability of xylanase: for the new era of biotechnology, J. Appl. Biol. Biotechnol. 11 (2023) 41–54, https://doi.org/10.7324/JABB.2023.110204.
[67] C. Li, A. Kumar, X. Luo, H. Shi, Z. Liu, G. Wu, Highly alkali-stable and cellulase-free xylanases from *Fusarium* sp. 21 and their application in clarification of orange juice, Int. J. Biol. Macromol. 155 (2020) 572–580, https://doi.org/10.1016/j.ijbiomac.2020.03.249.